Low-Complexity Joint Radar-Communication Beamforming: From Optimization to Deep Unfolding

Journal:	*Journal of Selected Topics in Signal Processing*
Manuscript ID	J-STSP-SPISC-00082-2023.R2
Manuscript Type:	Special Issue Paper (S1)
Date Submitted by the Author:	13-Aug-2024
Complete List of Authors:	Zhang, Jianjun; Nanjing University of Aeronautics and Astronautics; University College London Masouros, Christos; University College London, Electronic and Electrical Engineering Liu, Fan; Southern University of Science and Technology, Department of Electrical and Electronic Engineering; University College London, Department of Electronic and Electrical Engineering Huang, Yongming; Southeast University, School of Information Science and Engineering Swindlehurst, A. Lee; Dept. of Electrical and Computer Engineering, Electrical Engineering & Computer Science;

Low-Complexity Joint Radar-Communication Beamforming: From Optimization to Deep Unfolding

Jianjun Zhang, *Member, IEEE*, Christos Masouros, *Fellow, IEEE*
Fan Liu, *Senior Member, IEEE*, Yongming Huang, *Senior Member, IEEE*
and A. Lee Swindlehurst, *Fellow, IEEE*

***Abstract*—By sharing the same hardware platform, spectral resource as well as transmit waveform, dual-functional radar-communication (DFRC) systems have been envisioned as a key technology for the future wireless networks. However, advanced signal processing algorithms for DFRC, which can achieve better performance, tradeoff or other design goals, often suffer from prohibitive computational complexity. This motivates us to design low-complexity joint radar sensing and communication beamforming algorithms in this paper, so as to achieve better energy efficiency, communication-sensing tradeoff, and so on. First, we formulate the problem of joint radar-communication beamforming based on symbol-level precoding (SLP) by incorporating constructive interference so as to improve the energy efficiency. To address the formulated problem, we tailor highly parallelizable iterative optimization algorithms that are shown to converge to stationary (or locally optimal) points. To achieve better performance, we propose efficient recursive optimizations that monotonically improve the performance metric of interest. Simulation results indicate that the proposed iterative algorithms outperform the previous approaches. Finally, to further reduce the complexity, we employ deep unfolding to design efficient learning-based algorithms. Besides parallelizability, the learning-based algorithms also enjoy appealing advantages of scalability in the number of served users, the number of transmit antennas and the length of the radar pulse.**

***Index Terms*—Dual-functional radar-communication, symbol-level precoding, recursive optimization, sequential optimization, low-complexity design, integrated sensing and communication.**

I. Introduction

Integrated sensing and communication (ISAC) technology has attracted considerable attention recently, because it can significantly improve spectral and energy efficiency, reduce hardware cost and power consumption [1]–[3]. The integration of communication and radar sensing falls into two categories or levels, i.e., low-level loose integration and high-level tight integration [4], [5]. For the first category, the two functions are integrated in one system, but they use two sets of dedicated hardware components, and/or two different waveforms, superimposed or separated in time, frequency or spatial domains. In most cases, this low-level loose integration can only offer limited benefits, e.g., lower signalling overhead. As a step-change from the first one, the sensing and communication functions in the second category are more firmly integrated by sharing the majority of hardware components and are delivered by the same waveform, which is designed to optimize both communication and radar performance. A tightly integrated ISAC system is also referred to as a dual-functional radar-communication (DFRC) system in the literature [6].

Depending on the design priorities and underlying system priorities, current DFRC systems can be classified into three categories [4], i.e., communication-centric designs [7]–[10], radar-centric designs [11]–[13], and systems that are jointly designed and optimized [14]–[16]. In the first category, the design priority is communication, and the radar sensing is a secondary function. The main approach is to exploit communication waveforms to extract radar information via target echoes. For this design mode, a possible drawback is that the sensing performance is scenario-dependent and difficult-to-tune. On the contrary, a radar-centric design modulates information on a known radar waveform, which, for example, can be realized by integrating communication messages into radar waveforms via index modulation or by modulating radar sidelobes [17]. For this case, the performance loss in terms of radar sensing is negligible, since the radar signal remains largely unchanged. However, the main drawback is that the communication data rate is limited.

Compared to the first two categories, the joint design and optimization mode is the most flexible, facilitating a balance between the different design requirements for communication and radar sensing and offers a better trade-off between the two functions. Among various research problems, joint waveform optimization (WO) is pivotal to pursuing a desired performance tradeoff by choosing a performance metric to be optimized and constructing appropriate constraints [6], [11], [14]–[16], [18], [19], from both communication (e.g., SINR based constraints) and radar sensing (e.g., estimation accuracy). Many desired waveforms can be obtained by optimizing the

The work was supported by the Engineering and Physical Sciences Research Council, UK under project EP/S028455/1.

J. Zhang is with the College of Computer Science and Technology, Nanjing University of Aeronautics and Astronautics, Nanjing 211106, China (E-mail: jianjun.zhang@nuaa.edu.cn).

C. Masouros is with the Department of Electronic & Electrical Engineering, University College London, London WC1E7JE, U.K. (E-mail: c.masouros@ucl.ac.uk).

F. Liu is with the Department of Electronic and Electrical Engineering, Southern University of Science and Technology, Shenzhen 518055, China (Email: liuf6@sustech.edu.cn).

Y. Huang is with the National Mobile Communications Research Laboratory, Southeast University, Nanjing 210096, China (Email: huangym@seu.edu.cn).

A. Lee Swindlehurst is with the Center for Pervasive Communications and Computing, Henry Samueli School of Engineering, University of California at Irvine, Irvine, CA 92697 USA (Email: swindle@uci.edu).

spatial precoders, and three typical types within the proposed methods reviewed in [6] are mutual-information-based WO [20], [21], waveform (or beam-pattern) similarity-based WO [6], [14] and estimation-accuracy-based WO [22]–[24].

The principle of the first type lies in the fact that the mutual information measures the amount of information conveyed to the receiver by the propagation environment. A typical design methodology for the second type is to optimize the DFRC waveform to approximate an existing benchmark radar signal [6]. As for the third type, a WO problem can be formulated by constructing an optimization goal closely related to the accuracy of interest. A representative metric is the Cramér-Rao bound (CRB) of the estimated parameters, proposed recently in [23]. Note that in the previous works, the fully-connected array architecture is often assumed, which poses a large challenge for practical implementation. To tackle this issue, hardware-friendly hybrid beamforming algorithms are proposed in [17], [25], in which learning based solutions are also proposed. To enhance security, a secure beamforming scheme and a learning algorithm are proposed for a RIS-aided ISAC system [26].

It is well-known that one of the primary motivations for ISAC is to improve energy efficiency [5]. However, for most DFRC designs, conventional block-level precoding [27]–[29] is chosen to optimize the communication performance metrics, which fails to fully exploit the multi-user interference. A more recent line of research that has been developed for communication systems is symbol-level precoding (SLP). In contrast to the classical block-level precoding, where the interference is regarded as a harmful factor and is suppressed as much as possible, multi-user interference is instantaneously exploited in SLP. Typically, constructive interference (CI) is exploited to save the transmit power and therefore improve the energy efficiency. Examples using the concept of CI to improve communication system performance can be found in [30]–[36], in particular, the first work on optimization based low-complexity CI precoding [34]. Although SLP can exploit interference and improve energy efficiency, limited works have incorporated SLP into DFRC designs [37]–[40].

Although persistent efforts have been devoted to DFRC technology, practical applications have been handicapped by the prohibitive computational complexity. In contrast to most communication-only precoding/beamforming designs, space-time processing is often indispensable for ISAC radar sensing tasks. An immediate result of extending the signal processing to the time-dimension is that the resultant computational complexity becomes prohibitively high. To reduce the complexity, deep unfolding approach has been investigated and exploited in various radar applications [41]–[43]. In [41], the state-of-the-art algorithm designed via projection, descent, and retraction operations is unfolded to generate a deep network to address the problem of radar beam-pattern design. But DFRC waveform design problems typically require a large number of parameters, and the computational complexity of the space-time DFRC optimization increases dramatically as the length of the radar pulse or communication frame increases. If SLP is incorporated, this issue becomes more pronounced. The large computational complexity, caused by large problem scale and highly nonlinear form, is a key motivation of this paper.

In this paper, we first incorporate CI constraints into the problem of DFRC waveform optimization, so as to make full use of the multi-user interference to improve energy efficiency. To tackle the challenging issue of computational complexity and facilitate real-time implementation, we develop efficient parallelizable and recursive algorithms. The rationale for the recursive solution is based on the separability of the objective function, which means it can be broken down into a set of independent and smaller dimensional optimization problems. In particular, since the recursive algorithm monotonically improves the performance metric as the iterations proceed, it outperforms previous iterative algorithms which will have already converged to a stationary point. To further reduce the complexity, we employ deep unfolding to design a learning-based solution. These algorithms can make full use of parallel advantages of modern hardwares, e.g., GPU (graphics processing unit), and facilitate real-time implementation. The main contributions of our paper are summarized as follows:

- To exploit the multi-user interference and thus improve the energy efficiency of the DFRC system, we formulate the problem of joint radar-communication beamforming design based on SLP and, particularly, incorporate CI constraints into the problem of interest.
- To address the resulting non-convex optimization problem, we propose an efficient parallelizable iterative optimization algorithm, which can exploit latent separability of the optimization problem. We show that the proposed algorithm converges a locally optimal stationary point.
- In view of the space-time processing feature, we propose the idea of recursive optimization for SLP-based DFRC beamforming. For the considered problem, we propose an efficient recursive algorithm and reveal useful insights. In particular, we mathematically show that the proposed recursive algorithm monotonically improves the performance metric as the recursion proceeds.
- To further reduce the complexity, we propose efficient learning-based algorithms using deep-unfolding. Specifically, we first create unfolding-friendly iterative algorithms, and then unfold them by choosing the step-size parameters as the learnable parameters. In contrast to most learning-based algorithms, our algorithms enjoy the advantage of low training- and sample- complexity.

The integration gain of SLP and DFRC waveform optimization is at least three-fold, including better communication performance, sensing performance and performance tradeoff, but with reduced computational complexity. Comprehensive simulation results are provided to demonstrate these advantages. In particular, simulation results show that the number of required outer and inner iterations (or layers) is about 1/4 that of the original iterative algorithms.

The remainder of this paper is organized as follows. The problem formulation of DFRC WO design incorporating SLP is described in Section II. The parallelizable iterative optimization algorithm and deep-unfolding based learning solution are elaborated in Section III. In Section IV, the recursive design principle as well as the learning-based algorithm obtained using deep-unfolding and fractional programming is presented.

Useful insights are also provided to reveal appealing features of the recursive method. Simulation results and conclusions are given in Sections V and VI, respectively.

Notation: Bold uppercase and bold lowercase denote matrices and column vectors, respectively. Without particular specification, non-bold letters denote scalars. Caligraphic letters represent sets. $\mathbb{E}(\cdot)$ and $(\cdot)^{\mathrm{H}}$ denote the mathematical expectation and Hermitian operators, respectively. $\mathrm{card}(\cdot)$ and $\mathbb{I}\{\cdot\}$ represent the cardinality and the indicator function of a set, respectively. $(\cdot)^{\star}$ represents an optimal quantity, e.g., an optimal solution. $\mathcal{CN}(\mathbf{m},\mathbf{R})$ stands for a complex Gaussian random vector with mean $\mathbf{m}$ and covariance matrix $\mathbf{R}$.

II. System Model

Consider a MIMO DFRC base station (BS) equipped with N_{T} transmit antennas and N_{R} receive antennas, as shown in Fig. 1. The BS serves U single-antenna users (UEs), indexed by $\mathcal{U}=\{1,\cdots,U\}$. The channel vector between the BS and each UE $u\in\mathcal{U}$ is denoted by $\mathbf{h}_u\in\mathbb{C}^{N_{\mathrm{T}}\times 1}$. Let $\mathbf{X}\in\mathbb{C}^{N_{\mathrm{T}}\times L}$ be the DFRC signal matrix, where L is the length of the radar pulse or communication frame. For a practical system, L depends on a variety of factors, such as channel coherence, desired performance, implementation, and so on. Matrix $\mathbf{X}$ has dual identities. On the one hand, from the perspective of communication, x_{ij} (i.e., the (i,j)-th entry of $\mathbf{X}$) represents the discrete signal sample transmitted from antenna i at time-slot j. On the other hand, from the viewpoint of the radar, x_{ij} is the j-th fast-time snapshot transmitted from antenna i.

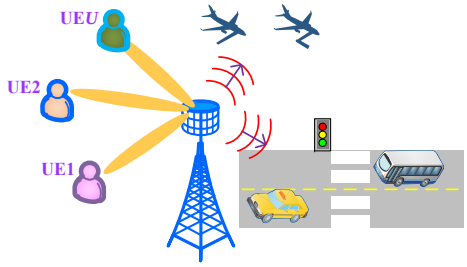

Fig. 1. An illustration of a dual-functional radar-communication system.

When $\mathbf{X}$ is transmitted by the BS, the signals received by the U UEs are given by

$$\mathbf{Y}_{\mathrm{C}}=\mathbf{H}\mathbf{X}+\mathbf{Z}_{\mathrm{C}}, \tag{1}$$

where $\mathbf{Z}_{\mathrm{C}}\in\mathbb{C}^{U\times L}$ is a matrix of received noise matrix whose columns are independent and distributed as $\mathcal{CN}(\mathbf{0},\sigma_{\mathrm{C}}^2\mathbf{I})$, and $\mathbf{H}=[\mathbf{h}_1,\mathbf{h}_2,\cdots,\mathbf{h}_U]^{\mathrm{H}}$ collects all of the UE channel vectors. Let $\mathbf{S}=[\mathbf{s}_1,\mathbf{s}_2,\cdots,\mathbf{s}_L]\in\mathbb{C}^{U\times L}$ collect all of the information symbols. The transmitted matrix $\mathbf{X}$ is a nonlinear function of the transmitted information symbols, i.e.,

$$\mathbf{X}=[\mathbf{x}_1,\mathbf{x}_2,\cdots,\mathbf{x}_L]=[\mathbf{x}_1(\mathbf{s}_1),\mathbf{x}_2(\mathbf{s}_2),\cdots,\mathbf{x}_L(\mathbf{s}_L)],$$

where $\mathbf{x}_i=\mathbf{x}_i(\mathbf{s}_i)$ is transmitted in time-slot i, and the i-th column of $\mathbf{Y}_{\mathrm{C}}$ (corresponding to $\mathbf{x}_i$) is used to recover $\mathbf{s}_i$. Note that the data matrix $\mathbf{S}$ is completely determined by the communication system (so that the problem in (6) optimizes the nonlinear mapping $\mathbf{X}$ for a fixed $\mathbf{S}$), and during the process we do not intervene in the operation of the communication system by controlling or modifying $\mathbf{S}$ in any way.

When $\mathbf{X}$ is transmitted to sense a target, the reflected echo signal matrix at the BS receiver can be written as

$$\mathbf{Y}_{\mathrm{R}}=\mathbf{G}\mathbf{X}+\mathbf{Z}_{\mathrm{R}}, \tag{2}$$

where, similar to $\mathbf{Z}_{\mathrm{C}}$ above, $\mathbf{Z}_{\mathrm{R}}$ denotes a matrix of received noise with each column independently distributed as $\mathcal{CN}(\mathbf{0},\sigma_{\mathrm{R}}^2\mathbf{I})$. The matrix $\mathbf{G}\in\mathbb{C}^{N_{\mathrm{R}}\times N_{\mathrm{T}}}$ in (2) represents the target response matrix. Typically, $\mathbf{G}$ can be expressed as

$$\mathbf{G}=\sum_{i=1}^{V}\alpha_i\mathbf{b}(\theta_i)\mathbf{a}^{\mathrm{H}}(\theta_i), \tag{3}$$

where $\alpha_i\in\mathbb{C}$ is the reflection coefficient (incorporating both path-loss and radar cross-section) of target i, θ_i is the azimuth angle of the target relative to the BS, V is the number of targets of interest, and $\mathbf{b}(\cdot)$ and $\mathbf{a}(\cdot)$ denote array response vectors that depend on the antenna array geometry.

Note that by changing value V in (3), response matrix $\mathbf{G}$ can characterize different scenarios. For clarity, we here take two specific examples to illustrate this point: 1) multiple point targets - V unstructured points that are far away from the BS like multiple UAVs; and 2) single extended target - the target is modeled as a surface with multiple distributed point-like scatterers, e.g., a vehicle moving on the road [23].

Without loss of generality, PSK modulation (with constellation $\mathcal{D}$ of size D is considered in this paper. The developed algorithms can be extended to other modulation modes. The (u,l)-th element of $\mathbf{S}$ is denoted by $s_{u,l}$. Let $s_{u,l}=e^{j\xi_{u,l}}\in\mathcal{D}$ be the intended PSK information symbol. The signal received at UE u in time-slot l can be written as

$$y_{u,l}=\mathbf{h}_u^{\mathrm{H}}\mathbf{x}_l+z_{u,l}, \tag{4}$$

where $\mathbf{x}_l$ denotes the l-th column of $\mathbf{X}$ and $z_{u,l}\sim\mathcal{CN}(0,\sigma_{\mathrm{C}}^2)$ denotes the received random noise.

To improve the energy efficiency, the idea of CI is exploited. For PSK modulation, the CI design principle can be captured by the following constraint $(\forall\, u,l)$ [36]

$$\begin{aligned}&\left|\mathrm{Im}(\mathbf{h}_u^{\mathrm{H}}\mathbf{x}_l e^{-j\xi_{u,l}})\right|\\&\quad\le\left(\mathrm{Re}(\mathbf{h}_u^{\mathrm{H}}\mathbf{x}_l e^{-j\xi_{u,l}})-\gamma_u\right)\tan(\pi/D),\end{aligned} \tag{5}$$

where the SNR metric γ_u measures the quality of the received signal. As shown in Fig. 2, the CI constraint pushes received signals away from the constellation decision boundaries, thereby improving the received SNR without the need to increase the transmit power [36] (See also [35] for more details).

In many cases, the Cramér-Rao bound (CRB) of specific parameters of interest is chosen as the performance metric to characterize the sensing performance, e.g., the direction cosine and radial velocity are considered in [44]. But similar to [23], the CRB of $\mathbf{G}$, instead of specific parameters, is chosen as the performance metric and optimization goal here. Essentially, we decouple or decompose a practical estimation task into two sub-tasks, i.e., the upstream task and downstream task. The upstream task is in charge of designing the transmit waveform $\mathbf{X}$, while the downstream task is responsible for estimating the specific parameters of interest. Moreover, if necessary, the

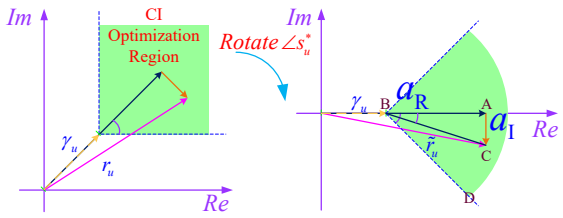

Fig. 2. The geometrical interpretation of CI constraint with QPSK modulation for $\xi = \pi/4$, where r_u represents noise-free received signal. The CI constraint requires that the noise-free received signal is within the CI region. To derive the CI condition, both r_u and CI region are rotated $\pi/4$ clockwise. For a general PSK constellation of size D, the angle rotated is equal to π/D. Let $\tilde{r}_u = r_u e^{-j\angle s_u} = r_u s_u^*$, $a_{\mathrm{R}} = \mathrm{Re}(\tilde{r}_u)$ and $a_{\mathrm{I}} = \mathrm{Im}(\tilde{r}_u)$. The CI condition holds if and only if $\angle ABD \geq \angle ABC$. Note that due to the monotonicity of the tan function in $(0, \pi/2)$, this condition is equivalent to $\tan(\angle ABD) \geq \tan(\angle ABC) = |a_{\mathrm{I}}/(a_{\mathrm{R}} - \gamma)|$, which is, in fact, the expression in (5).

receiver techniques should also be taken into account in the downstream task to improve the estimation quality.

The reasons to decompose a practical estimation task into two sub-tasks are as follows. First and foremost, the BS often has no prior knowledge about the number of scatterers or targets and different applications often have different estimation objectives. Second, to derive an analytic expression of CRB for specific parameters, the techniques used by the receiver often have to be taken into account, which complicates the design of $\mathbf{X}$ and limits the application scope. Finally, if $\mathbf{G}$ can be well estimated, sophisticated array signal processing algorithms can be later invoked to extract the information of interest from $\mathbf{G}$, e.g., the parameters like angles and reflection coefficients can be extracted from $\mathbf{G}$ via the MUSIC and APES algorithms.

For the upstream task here, the key is to optimize transmit waveform $\mathbf{X}$, which makes the estimation of $\mathbf{G}$ both accurate and simple. Given the linear signal model $\mathbf{Y}_{\mathrm{R}} = \mathbf{G}\mathbf{X} + \mathbf{Z}_{\mathrm{R}}$, an estimator of $\mathbf{G}$, which is calculated easily, can be obtained via the pseudo-inverse method, i.e., $\hat{\mathbf{G}} = \mathbf{Y}_{\mathrm{R}}\mathbf{X}^{\mathrm{H}}\big(\mathbf{X}\mathbf{X}^{\mathrm{H}}\big)^{-1}$. It can be verified that the estimator $\hat{\mathbf{G}}$ is unbiased, i.e., $\mathbb{E}(\hat{\mathbf{G}}) = \mathbf{G}$, with mean square error (MSE) $N_{\mathrm{R}}\sigma_{\mathrm{R}}^2 \mathrm{tr}\big(\mathbf{X}\mathbf{X}^{\mathrm{H}}\big)^{-1}$. It can also be verified that the MSE of $\hat{\mathbf{G}}$ and the CRB of $\mathbf{G}$ coincide, which shows that the estimator is efficient and, in some sense, optimal [45], as the MSE attains CRB. Hence, the design goal in this paper is to optimize $\mathbf{X}$ by minimizing the MSE of $\hat{\mathbf{G}}$ or the CRB of $\mathbf{G}$ subject to the constraints on communication quality and transmit power, which can be formulated as

$$\begin{aligned} \min_{\mathbf{X}} \quad & \mathrm{tr}\big((\mathbf{X}\mathbf{X}^{\mathrm{H}})^{-1}\big) \\ \text{s.t.} \quad & \big|\mathrm{Im}(\mathbf{h}_u^{\mathrm{H}}\mathbf{x}_l e^{-j\xi_{u,l}})\big| \leq \\ & \qquad \big(\mathrm{Re}(\mathbf{h}_u^{\mathrm{H}}\mathbf{x}_l e^{-j\xi_{u,l}}) - \gamma_u\big)C_\pi, \ (\forall\, u, l) \\ & \|\mathbf{x}_l\|^2 \leq p, \ (\forall\, l), \end{aligned} \tag{6}$$

where p denotes the maximum transmit power for each symbol vector, and $C_\pi = \tan(\pi/D)$.

Note that besides the non-convex objective in problem (6), the most difficult challenge is the large scale of the problem, in terms of both large size of optimization variable and large number of constraints. In particular, the computational complexity of optimizing over the matrix $\mathbf{X}$ is often prohibitively high, which makes it challenging to implement in real-time. Moreover, as the dimensions of matrix $\mathbf{X}$ increase (e.g., as L increases), this issue becomes more pronounced. In what follows, we will tackle the above issue by designing efficient parallelizable and recursive algorithms from the point of view of both optimization and learning. [1]

III. Parallelizable Beamforming Design

In this section, we propose efficient parallelizable algorithms that exploit the separability of the CI constraints.

A. Optimization-based Parallelizable Beamforming Design

The non-convexity of the objective in problem (6) prevents efficient solving. To tackle this issue, we use the first-order approximation method and first derive the (complex) conjugate gradient of $\mathrm{tr}\big((\mathbf{X}\mathbf{X}^{\mathrm{H}})^{-1}\big)$. For the sake of convenience, let $f(\mathbf{X}) = \mathrm{tr}\big((\mathbf{X}\mathbf{X}^{\mathrm{H}})^{-1}\big)$. The (complex) conjugate gradient of $f(\mathbf{X})$ is denoted by $\partial f/\partial \mathbf{X}^{\mathrm{H}}$, which can be obtained using the matrix differential as follows [46]:

$$\begin{aligned} df(\mathbf{X}) &= -\mathrm{tr}\big((\mathbf{X}\mathbf{X}^{\mathrm{H}})^{-1} d(\mathbf{X}\mathbf{X}^{\mathrm{H}})(\mathbf{X}\mathbf{X}^{\mathrm{H}})^{-1}\big) \\ &= -\mathrm{tr}\big((\mathbf{X}\mathbf{X}^{\mathrm{H}})^{-2}(d\mathbf{X}\cdot\mathbf{X}^{\mathrm{H}} + \mathbf{X}\cdot d\mathbf{X}^{\mathrm{H}})\big) \\ &= -\mathrm{tr}\big(\mathbf{X}^{\mathrm{H}}(\mathbf{X}\mathbf{X}^{\mathrm{H}})^{-2} d\mathbf{X} + (\mathbf{X}\mathbf{X}^{\mathrm{H}})^{-2}\mathbf{X} d\mathbf{X}^{\mathrm{H}}\big). \end{aligned} \tag{7}$$

As per the identification theorem of the matrix differential, we can obtain the gradient of f with respect to $\mathbf{X}$ [46]

$$\partial f/\partial \mathbf{X}^{\mathrm{H}} = (\mathbf{X}\mathbf{X}^{\mathrm{H}})^{-2}\mathbf{X}. \tag{8}$$

Let $\mathbf{X}_n$ represent the n-th iteration of variable $\mathbf{X}$. Due to (7) and (8), the objective function can be expressed as

$$\begin{aligned} &\mathrm{tr}\big((\mathbf{X}\mathbf{X}^{\mathrm{H}})^{-1}\big) = \mathrm{tr}\big((\mathbf{X}_n\mathbf{X}_n^{\mathrm{H}})^{-1}\big) - \\ &\quad 2\mathrm{Re}\big(\mathrm{tr}\big((\mathbf{X}_n\mathbf{X}_n^{\mathrm{H}})^{-2}\mathbf{X}_n\mathbf{X}^{\mathrm{H}}\big)\big) + o(\|\mathbf{X} - \mathbf{X}_n\|^2). \end{aligned} \tag{9}$$

Using the first-order method yields the following problem [47]

$$\begin{aligned} \min_{\mathbf{X}} \quad & -\mathrm{Re}\big(\mathrm{tr}\big((\mathbf{X}_n\mathbf{X}_n^{\mathrm{H}})^{-2}\mathbf{X}_n\mathbf{X}^{\mathrm{H}}\big)\big) \\ \text{s.t.} \quad & \big|\mathrm{Im}(\mathbf{h}_u^{\mathrm{H}}\mathbf{x}_l e^{-j\xi_{u,l}})\big| \leq \\ & \qquad \big(\mathrm{Re}(\mathbf{h}_u^{\mathrm{H}}\mathbf{x}_l e^{-j\xi_{u,l}}) - \gamma_u\big)C_\pi, \ (\forall\, u, l) \\ & \|\mathbf{x}_l\|^2 \leq p, \ (\forall\, l). \end{aligned} \tag{10}$$

To accelerate convergence, a quadratic penalty term is added to the approximate objective function with penalty parameter $\rho_n > 0$ [48], [49]:

$$\begin{aligned} \min_{\mathbf{X}} \quad & -\mathrm{Re}\big(\mathrm{tr}\big((\mathbf{X}_n\mathbf{X}_n^{\mathrm{H}})^{-2}\mathbf{X}_n\mathbf{X}^{\mathrm{H}}\big)\big) + \frac{\rho_n}{2}\|\mathbf{X} - \mathbf{X}_n\|_{\mathrm{F}}^2 \\ \text{s.t.} \quad & \big|\mathrm{Im}(\mathbf{h}_u^{\mathrm{H}}\mathbf{x}_l e^{-j\xi_{u,l}})\big| \leq \\ & \qquad \big(\mathrm{Re}(\mathbf{h}_u^{\mathrm{H}}\mathbf{x}_l e^{-j\xi_{u,l}}) - \gamma_u\big)C_\pi, \ (\forall\, u, l) \\ & \|\mathbf{x}_l\|^2 \leq p, \ (\forall\, l). \end{aligned} \tag{11}$$

The rationale for the penalty function is that as the solution approaches its optimal value, the objective function becomes strongly convex, and the convergence is accelerated.

Before proceeding, note that in contrast to the well-known majorization-minimization technique [50], which requires that

[1] In general, deep learning, e.g., deep unfolding, can be exploited to enhance an optimization algorithm by improving communication performance metrics or reduce computational complexities. We focus on the latter in this paper.

the surrogate objective must upper bound the original objective, this condition is not required by the algorithms derived in this paper [47]. Note also that theoretically the matrix variable $\mathbf{X}$ may be rank-deficient due to the first-order approximation. If necessary, the phenomenon of rank-defect can be detected or monitored via checking or tracking the condition number or objective function value. But in practice, this phenomenon has not yet been observed, maybe thanks to the CI constraints and quadratic term, which shows its safety and validity.

Although problem (11) can be solved directly, it can be handled more efficiently. For the sake of convenience, we define $\mathbf{C}_n$ and explicitly write $\mathbf{X}_n$ as

$$\begin{aligned}\mathbf{C}_n =&(\mathbf{X}_n\mathbf{X}_n^{\mathrm{H}})^{-2}\mathbf{X}_n = [\mathbf{c}_1, \mathbf{c}_2, \cdots, \mathbf{c}_L]\\ \mathbf{X}_n =&[\mathbf{x}_{1,n}, \mathbf{x}_{2,n}, \cdots, \mathbf{x}_{L,n}].\end{aligned}$$

Since problem (11) is separable, it can be broken into L independent sub-problems with respect to each column $\mathbf{x}_l$ of $\mathbf{X}$. Specifically, the l-th sub-problem is given by

$$\begin{aligned}\min_{\mathbf{x}_l} \quad & -\mathrm{Re}\big(\mathbf{x}_l^{\mathrm{H}}\mathbf{c}_l\big) + \frac{\rho_n}{2}\|\mathbf{x}_l - \mathbf{x}_{l,n}\|^2\\ \text{s.t.} \quad & \big|\mathrm{Im}(\mathbf{h}_u^{\mathrm{H}}\mathbf{x}_l e^{-j\xi_{u,l}})\big| \le \\ & \qquad \big(\mathrm{Re}(\mathbf{h}_u^{\mathrm{H}}\mathbf{x}_l e^{-j\xi_{u,l}}) - \gamma_u\big)C_\pi,\ (\forall\, u)\\ & \|\mathbf{x}_l\|^2 \le p.\end{aligned} \tag{12}$$

Compared to problem (6), the dimension of the optimization variable for each sub-problem in (12) is much smaller and can be solved more efficiently. This advantage becomes more pronounced as L increases. Moreover, because the separability of the CI constraints is exploited, the algorithm can be implemented in parallel, which has further computational advantages. Since problem (11) (or (12)) is convex, it can be solved using standard convex tools, e.g., CVXOPT.

Algorithm 1: Optimization Algorithm for Problem (6)

1: **initialize:** optimization variable $\mathbf{X}_0$ and parameter ρ_n

2: **repeat**

(a) **construct** convex optimization problem (11)

(b) **solve** the constructed optimization problem

3: **until** some convergence criterion is met

4: **output:** (locally optimal) transmit matrix $\mathbf{X}^\star$

The complete iterative procedure is summarized in Algorithm 1.The computational complexity of solving problem (12) is denoted by C, which depends on a specific optimization solver. Then, the computational complexity of Algorithm 1 is dominated by LCD, with D denoting the number of iterations in Algorithm 1. To guarantee that the iterative algorithm can converge, the relatively conservative hyper-parameters, e.g., $\{\rho_n\}$, are chosen first, which can be later optimized via deep-unfolding. The optimization variable $\mathbf{X}$ is initialized first in step 1. A convex optimization problem is constructed first in step (a) and then solved in step (b). This procedure is repeated until a convergence criterion is met. A typical convergence criterion is $\|\mathbf{X}_n - \mathbf{X}_{n-1}\| \le \varepsilon$, where $\varepsilon > 0$ is a small real number. Algorithm 1 designed to solve problem (6) converges to a stationary point, as shown in the following theorem.

Theorem 1. *Let $\{\mathbf{X}_n\}$ be the sequence of estimates generated by Algorithm 1. Then, every limit point of $\{\mathbf{X}_n\}$ is a stationary point.*

Proof: For brevity, the feasible set of problem (11), which is closed and convex, is denoted by $\mathcal{F}$, i.e.,

$$\begin{aligned}\mathcal{F} = \Big\{\mathbf{X}\,\Big|\, \|\mathbf{x}_l\|^2 \le & p, (\forall\, l), \quad \big|\mathrm{Im}(\mathbf{h}_u^{\mathrm{H}}\mathbf{x}_l e^{-j\xi_{u,l}})\big| \le \\ & \big(\mathrm{Re}(\mathbf{h}_u^{\mathrm{H}}\mathbf{x}_l e^{-j\xi_{u,l}}) - \gamma_u\big)C_\pi, (\forall\, u, l)\Big\}.\end{aligned}$$

Then, problem (11) can be equivalently written as

$$\begin{aligned}\min_{\mathbf{X}} \quad & \|\mathbf{X} - \mathbf{X}_n - \mathbf{C}_n/\rho_n\|_{\mathrm{F}}^2\\ \text{s.t.} \quad & \mathbf{X} \in \mathcal{F}.\end{aligned} \tag{13}$$

According to the definition of projection in a Euclidean space [2], the optimal solution of problem (13), denoted by $\mathbf{X}_{n+1}$, can be compactly expressed as

$$\mathbf{X}_{n+1} = \mathrm{Proj}_{\mathcal{F}}(\mathbf{X}_n + \mathbf{C}_n/\rho_n). \tag{14}$$

Under some step-size criterion or rule [3], the convergence of the iteration in (14) can be obtained immediately, e.g., by invoking Proposition 2.3.3 in [47]. ■

Although the proposed iterative algorithm can converge to a stationary point, it still suffers from several drawbacks. First, the preassigned hyper-parameters, e.g., the penalty parameters $\{\rho_n\}$ and the step-sizes used to solve problem (12), critically determine the convergence rate. However, it is challenging to choose them optimally using conventional methods such as convergence analysis. Second, computation-intensive operations such as the matrix inversion in (11) exacerbate the computational complexity. Next, we propose a learning-based algorithm to tackle these issues.

B. Low-Complexity Implementation via Deep Unfolding

To address the aforementioned issues, we employ the deep unfold technique to design a learning-based algorithm. Deep unfolding, which belongs to the category of model-based deep learning, unfolds the iterations of an existing iterative algorithm into a neural-network-analogous layer-wise structure and optimizes the relevant hyper-parameters via gradient descent and back-propagation methods. Besides the advantages of optimizing important hyper-parameters (which are often chosen heuristically in practice) and thus accelerating convergence, the other motivations of incorporating deep unfolding include small-sample performance and good interpretability [51].

Note that although deep unfolding is an appealing technique, most existing iterative algorithms are unfolding-friendly, i.e., the iteration operations within an iterative algorithm contain the operations that prevent the back propagation method from training the resulting deep algorithmic network. In fact, off-the-shelf solvers are typically unfriendly to unfolding, e.g., the interior-point method consists of a complicated backtracking

[2]The projection of a point $\boldsymbol{x}$ on a closed convex set $\mathcal{C}$, denoted by $\boldsymbol{x}^\star$, is defined as $\boldsymbol{x}^\star \triangleq \mathrm{Proj}_{\mathcal{C}}(\boldsymbol{x}) = \arg\min_{\boldsymbol{y}\in\mathcal{C}} ||\boldsymbol{y}-\boldsymbol{x}||^2$ (Appendix B of [47]).

[3]Note that although the expression in (14) is brief and compact, a closed-form solution is still unavailable. Hence, an iterative algorithm has to be invoked to tackle it, which involves the step-size parameter. Various step-size rules have been available, such as the Armijo or Goldstein rules [47].

line search. Moreover, the power constraint $\|\mathbf{x}_l\|^2 \le p$ and the CI constraints are inhomogeneous, which should be distinguished and treated differently in order to obtain a more efficient algorithm. Due to these factors, we will design an unfolding-friendly algorithm that solves problem (12).

To distinguish and more efficiently tackle the two types of constraints and exploit latent separability, we will exploit duality. Specifically, we introduce an auxiliary optimization variable $\mathbf{z}_l$ and equivalently write problem (12) as

$$\begin{aligned} \min_{\mathbf{x}_l,\mathbf{z}_l} \quad & -\mathrm{Re}\big(\mathbf{x}_l^{\mathrm{H}}\mathbf{c}_l\big) + \frac{\rho_n}{2}\|\mathbf{x}_l - \mathbf{x}_{l,n}\|^2 \\ \text{s.t.} \quad & \big|\mathrm{Im}(\mathbf{h}_u^{\mathrm{H}}\mathbf{z}_l e^{-j\xi_{u,l}})\big| \le \\ & \qquad \big(\mathrm{Re}(\mathbf{h}_u^{\mathrm{H}}\mathbf{z}_l e^{-j\xi_{u,l}}) - \gamma_u\big)C_\pi,\ (\forall\, u) \\ & \mathbf{x}_l = \mathbf{z}_l, \quad \|\mathbf{x}_l\|^2 \le p. \end{aligned} \tag{15}$$

The augmented Lagrangian with respect to equality constraint $\mathbf{x}_l = \mathbf{z}_l$ of problem (15) is given by [47]

$$\begin{aligned} \min_{\mathbf{x}_l,\mathbf{z}_l} \quad & -\mathrm{Re}\big(\mathbf{x}_l^{\mathrm{H}}\mathbf{c}_l\big) + \frac{\rho_n}{2}\|\mathbf{x}_l - \mathbf{x}_{l,n}\|^2 \\ & \quad + \mathrm{Re}\big((\mathbf{x}_l - \mathbf{z}_l)^{\mathrm{H}}\mathbf{y}_l\big) + \frac{\kappa}{2}\|\mathbf{x}_l - \mathbf{z}_l\|^2 \\ \text{s.t.} \quad & \big|\mathrm{Im}(\mathbf{h}_u^{\mathrm{H}}\mathbf{z}_l e^{-j\xi_{u,l}})\big| \le \\ & \qquad \big(\mathrm{Re}(\mathbf{h}_u^{\mathrm{H}}\mathbf{z}_l e^{-j\xi_{u,l}}) - \gamma_u\big)C_\pi,\ (\forall\, u) \\ & \|\mathbf{x}_l\|^2 \le p, \end{aligned} \tag{16}$$

where $\mathbf{y}_l$ denotes the dual variable for constraint $\mathbf{x}_l = \mathbf{z}_l$ and $\kappa > 0$ is the penalty parameter. By constructing a serial of sub-problems taking the form of (16) and solving them exactly or inexactly, these solutions finally converge to the same globally optimal solution of problem (15) or (12) in terms of $\mathbf{x}_l$.

To solve problem (16), we alternatively solve the following two sub-problems and update the dual variable $\mathbf{y}_l$.

1) Sub-problem with respect to (w.r.t.) variable $\mathbf{x}_l$: To update $\mathbf{x}_l$, it is sufficient to solve the following problem

$$\begin{aligned} \min_{\mathbf{x}_l} \quad & -\mathrm{Re}\big(\mathbf{x}_l^{\mathrm{H}}\mathbf{c}_l\big) + \frac{\rho_n}{2}\|\mathbf{x}_l - \mathbf{x}_{l,n}\|^2 \\ & \quad + \mathrm{Re}\big((\mathbf{x}_l - \mathbf{z}_l)^{\mathrm{H}}\mathbf{y}_l\big) + \frac{\kappa}{2}\|\mathbf{x}_l - \mathbf{z}_l\|^2 \\ \text{s.t.} \quad & \|\mathbf{x}_l\|^2 \le p. \end{aligned} \tag{17}$$

Note that problem (17) can be solved analytically. Defining $\bar{\mathbf{x}}_l = (\rho_n + \kappa)^{-1}(\mathbf{c}_l + \rho_n\mathbf{x}_{l,n} - \mathbf{y}_l + \kappa\mathbf{z}_l)$, the closed-form optimal solution, denoted by $\mathbf{x}_{l,n}^\star$, is given by

$$\mathbf{x}_{l,n}^\star = \begin{cases} \bar{\mathbf{x}}_l & \text{if } \|\bar{\mathbf{x}}_l\|^2 \le p \\ \sqrt{p}\bar{\mathbf{x}}_l/\|\bar{\mathbf{x}}_l\| & \text{otherwise.} \end{cases} \tag{18}$$

2) Sub-problem w.r.t. variable $\mathbf{z}_l$: The optimization variable $\mathbf{z}_l$ is updated by solving the following problem

$$\begin{aligned} \min_{\mathbf{z}_l} \quad & \mathrm{Re}\big((\mathbf{x}_l - \mathbf{z}_l)^{\mathrm{H}}\mathbf{y}_l\big) + \frac{\kappa}{2}\|\mathbf{x}_l - \mathbf{z}_l\|^2 \\ \text{s.t.} \quad & \big|\mathrm{Im}(\mathbf{h}_u^{\mathrm{H}}\mathbf{z}_l e^{-j\xi_{u,l}})\big| \le \\ & \qquad \big(\mathrm{Re}(\mathbf{h}_u^{\mathrm{H}}\mathbf{z}_l e^{-j\xi_{u,l}}) - \gamma_u\big)C_\pi,\ (\forall\, u). \end{aligned} \tag{19}$$

Problem (19) is convex and can be solved via standard tools. However, the underlying algorithm is not unfolding-friendly. Later on, we will propose an unfolding-friendly version.

Finally, we update the dual variable $\mathbf{y}_l$ in the t-th iteration as

$$\mathbf{y}_{l,t} = \mathbf{y}_{l,t-1} + \kappa(\mathbf{x}_{l,t} - \mathbf{z}_{l,t}), \tag{20}$$

where $\mathbf{y}_{l,t}$ represents the t-th iteration of $\mathbf{y}_l$. Based on the above, we obtain the novel approach summarized in Algorithm 2, which is also guaranteed to converge to a stationary point.

Algorithm 2: Iterative Algorithm for Problem (12)

1: **initialize:** dual variable $\mathbf{y}_{l,0}$, auxiliary variable $\mathbf{z}_{l,0}$ and penalty parameter κ

2: **repeat**

(a) **update** primal variable $\mathbf{x}_l$ according to (18)

(b) **update** auxiliary variable $\mathbf{z}_l$ by solving (19)

(c) **update** dual variable $\mathbf{y}_l$ according to (20)

3: **until** some convergence criterion is met

4: **output:** transmit vector $\mathbf{x}_l^\star$

Next, we further unfold the obtained iterative algorithm. For sub-problem (17), a closed-form solution is available, so we need to design an algorithm to solve sub-problem (19). Let $\mathbf{z}_l = \bar{\mathbf{z}}_{\mathrm{R},l} + j\bar{\mathbf{z}}_{\mathrm{I},l}$ and $e^{j\xi_{u,l}}\mathbf{h}_u = \bar{\mathbf{h}}_{\mathrm{R},u,l} + j\bar{\mathbf{h}}_{\mathrm{I},u,l}$, where $\bar{\mathbf{z}}_{\mathrm{R},l}$ and $\bar{\mathbf{z}}_{\mathrm{I},l}$ represent the real and imaginary part of complex variable $\mathbf{z}_l$. The (real) vectors $\bar{\mathbf{h}}_{\mathrm{R},u,l}$ and $\bar{\mathbf{h}}_{\mathrm{I},u,l}$ are similarly defined. For convenience, we let $\mathbf{x}_l + \mathbf{y}_l/\kappa = \mathbf{v}_{\mathrm{R},l} + j\mathbf{v}_{\mathrm{I},l}$ and define vectors $\mathbf{w}_l$, $\mathbf{q}_l$, $\{\mathbf{a}_{u,l}\}$ and $\{\mathbf{b}_{u,l}\}$ as follows:

$$\begin{aligned} \mathbf{w}_l^{\mathrm{T}} &= [\bar{\mathbf{z}}_{\mathrm{R},l}^{\mathrm{T}}, \bar{\mathbf{z}}_{\mathrm{I},l}^{\mathrm{T}}], \quad \mathbf{q}_l^{\mathrm{T}} = [\mathbf{v}_{\mathrm{R},l}^{\mathrm{T}}, \mathbf{v}_{\mathrm{I},l}^{\mathrm{T}}] \\ \mathbf{a}_{u,l}^{\mathrm{T}} &= \big[C_u\bar{\mathbf{h}}_{\mathrm{R},u,l}^{\mathrm{T}} + \bar{\mathbf{h}}_{\mathrm{I},u,l}^{\mathrm{T}}, C_u\bar{\mathbf{h}}_{\mathrm{I},u,l}^{\mathrm{T}} - \bar{\mathbf{h}}_{\mathrm{R},u,l}^{\mathrm{T}}\big],\ (\forall\, u) \\ \mathbf{b}_{u,l}^{\mathrm{T}} &= \big[C_u\bar{\mathbf{h}}_{\mathrm{R},u,l}^{\mathrm{T}} - \bar{\mathbf{h}}_{\mathrm{I},u,l}^{\mathrm{T}}, C_u\bar{\mathbf{h}}_{\mathrm{I},u,l}^{\mathrm{T}} + \bar{\mathbf{h}}_{\mathrm{R},u,l}^{\mathrm{T}}\big],\ (\forall\, u). \end{aligned}$$

Then, problem (19) can be equivalently expressed as

$$\begin{aligned} \min_{\mathbf{w}_l} \quad & \mathbf{w}_l^{\mathrm{T}}\mathbf{w}_l/2 - \mathbf{w}_l^{\mathrm{T}}\mathbf{q}_l \\ \text{s.t.} \quad & \mathbf{a}_{u,l}^{\mathrm{T}}\mathbf{w}_l \ge C_u\gamma_u,\ \mathbf{b}_{u,l}^{\mathrm{T}}\mathbf{w} \ge C_u\gamma_u,\ (\forall\, u). \end{aligned} \tag{21}$$

The Lagrangian of problem (21) is given by

$$\begin{aligned} L(\mathbf{w}_l, \boldsymbol{\mu}_l, \boldsymbol{\lambda}_l) = & \frac{1}{2}\mathbf{w}_l^{\mathrm{T}}\mathbf{w}_l - \mathbf{q}_l^{\mathrm{T}}\mathbf{w}_l \\ & + \sum_{u\in\mathcal{U}} \mu_{u,l}(C_u\gamma_u - \mathbf{a}_{u,l}^{\mathrm{T}}\mathbf{w}_l) \\ & + \sum_{u\in\mathcal{U}} \lambda_{u,l}(C_u\gamma_u - \mathbf{b}_{u,l}^{\mathrm{T}}\mathbf{w}_l), \end{aligned} \tag{22}$$

where $\mu_{u,l}(\ge 0)$ and $\lambda_{u,l}(\ge 0)$ denote the dual variables for the inequality constraints. Solving problem (21) via the primal-dual method boils down to the following iterations:

$$\mathbf{w}_l \leftarrow \mathbf{q}_l + \sum_{u\in\mathcal{U}} \mu_{u,l}\mathbf{a}_{u,l} + \sum_{u\in\mathcal{U}} \lambda_{u,l}\mathbf{b}_{u,l} \tag{23}$$

$$\mu_{u,l} \leftarrow \max\big\{\mu_{u,l} + \alpha(C_u\gamma_u - \mathbf{a}_{u,l}^{\mathrm{T}}\mathbf{w}_l), 0\big\} \tag{24}$$

$$\lambda_{u,l} \leftarrow \max\big\{\lambda_{u,l} + \alpha(C_u\gamma_u - \mathbf{b}_{u,l}^{\mathrm{T}}\mathbf{w}_l), 0\big\}, \tag{25}$$

where $\alpha(>0)$ denotes the step-size parameter [4].

Updating $\mathbf{X}$ involves matrix inversion $(\mathbf{X}_n\mathbf{X}_n^{\mathrm{H}})^{-2}$, which prevents efficient unfolding due to resulting high complexity. Next, we tackle this issue. Let $\boldsymbol{\Lambda}$ denote the diagonal matrix

[4]Since the CI constraints are homogeneous, the dual variables can share the same step-size parameter α without impacting the convergence performance.

obtained by extracting the diagonal elements of $\mathbf{X}_n\mathbf{X}_n^{\mathrm{H}}$. Then, matrix $\mathbf{X}_n\mathbf{X}_n^{\mathrm{H}}$ can be written as $\mathbf{X}_n\mathbf{X}_n^{\mathrm{H}} = \mathbf{Q} + \mathbf{\Lambda}$ with $\mathbf{Q} = \mathbf{X}_n\mathbf{X}_n^{\mathrm{H}} - \mathbf{\Lambda}$. Now, $(\mathbf{X}_n\mathbf{X}_n^{\mathrm{H}})^{-1}$ can be approximated by

$$\begin{aligned}(\mathbf{Q}+\mathbf{\Lambda})^{-1} =& \mathbf{\Lambda}^{-1}\left(\mathbf{I} + \sum_{n=1}^{\infty}(-1)^n\left(\mathbf{Q}\mathbf{\Lambda}^{-1}\right)^n\right) \\ \overset{(*)}{\approx}& \mathbf{\Lambda}^{-1} - \mathbf{\Lambda}^{-1}\mathbf{Q}\mathbf{\Lambda}^{-1} + \mathbf{\Lambda}^{-1}\mathbf{Q}\mathbf{\Lambda}^{-1}\mathbf{Q}\mathbf{\Lambda}^{-1}, \quad (26)\end{aligned}$$

where $(*)$ is obtained by omitting all terms greater than order $n = 3$. To reduce possible errors caused by the approximation above, we introduce a trainable matrix parameter $\mathbf{V}$, i.e.,

$$(\mathbf{X}_n\mathbf{X}_n^{\mathrm{H}})^{-1} = \mathbf{\Lambda}^{-1} - \mathbf{\Lambda}^{-1}\mathbf{Q}\mathbf{\Lambda}^{-1} + \mathbf{\Lambda}^{-1}\mathbf{Q}\mathbf{\Lambda}^{-1}\mathbf{Q}\mathbf{\Lambda}^{-1} + \mathbf{V}.$$

The updates in (23) - (25) can be implemented in parallel for each l. In particular, the most complex and time-consuming operation within these updates is the inner product between two vectors, whose computational complexity is $\mathcal{O}(N_{\mathrm{T}})$. Thanks to the closed-form solution in (18) and the parallelizability, the proposed algorithm can be applied to large-scale multi-antenna systems. The benefits are attributed to the fact that the separability is efficiently exploited.

Based on (18), (20) and (23) - (26), we can unfold Algorithm 1. The structure of the unfolded deep network is depicted in Fig. 3. The deep network consists of N layers, and each layer consists of 3 sub-layers whose forward propagation (FP) formulas are provided in (18), (20) and (23) - (25), and also shown in Fig. 3. The trainable or learnable parameters are collected in $\mathbf{\Theta} = \{\mathbf{V}_n, \rho_n, \kappa_{n,t}, \alpha_{n,t,k} \,|\, n = 1, \cdots, N, t = 1, \cdots, T, k = 1, \cdots, K\}$, where $\mathbf{V}_n$ is the matrix parameter within the n-th layer, ρ_n is the projection step-size parameter for the n-th layer, $\kappa_{n,t}$ is the step-size parameter for the iteration in (20), and $\alpha_{n,t,k}$ is the step-size parameter used by the k-th update in (24) and (25) of the t-th sub-layer within the n-th layer.

Mathematically, the above deep network can be regarded as a mapping, which we denote by $\mathcal{G}(\cdot, \mathbf{\Theta})$. The input to $\mathcal{G}(\cdot)$ includes CSI $\{\mathbf{h}_u\}$ and transmitted symbol matrix $\mathbf{S}$, which are collected in $\mathcal{X} = \{\mathbf{h}_u, \mathbf{S} \,|\, u \in \mathcal{U}\}$. Given a training sample $(\mathcal{X}_i, \mathbf{X}_i)$ with $\mathbf{X}_i$ denoting the label, the FP predicts an output $\mathcal{G}(\mathcal{X}_i, \mathbf{\Theta})$, and the loss can be calculated as

$$L(\mathcal{X}_i, \mathbf{X}_i) = \|\mathbf{X}_i - \mathcal{G}(\mathcal{X}_i, \mathbf{\Theta})\|^2. \quad (27)$$

Then, $\mathbf{\Theta}$ can be updated via back-propagation (BP). Since all mathematical operations within $\mathcal{G}(\cdot, \mathbf{\Theta})$ (e.g., the update in (23) - (25)) are differentiable or at least differentiable almost everywhere, the required gradients can be calculated via the chain rules or automatic differentiation methods provided by deep learning libraries such as Tensorflow or Pytorch.

For clarity, the training procedure is summarized in Algorithm 3. The most important input is the training dataset used for training the deep network. The elements of the training dataset can be obtained via Algorithm 1 or 4. Before training the network, the learnable parameters are initialized randomly in step 2. Within each training epoch, a batch of training samples are chosen randomly from the dataset in step 3-(a), and then fed to the network to generate predictions in step 3-(b). With the predictions available, the loss can be calculated in step 3-(c) and used to update the trainable parameters in step 3-(d). When the training procedure is finished, we can obtain the optimal parameters. The use of the trained network is straightforward and is omitted here.

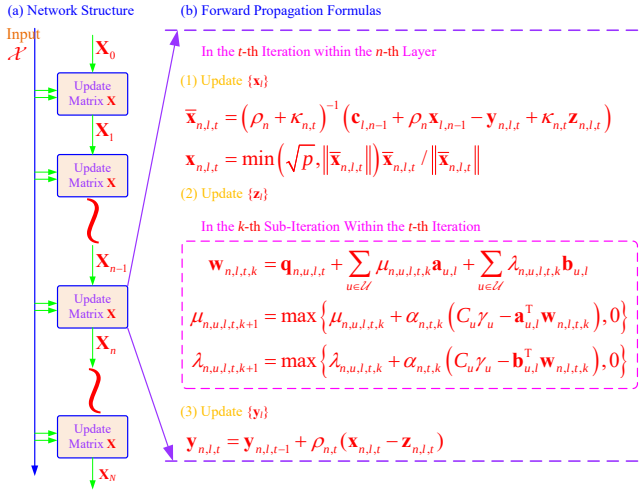

Fig. 3. The network structure and forward propagation formulas of the deep network derived from the iterative optimization algorithm.

Algorithm 3: Beamforming Design via Learning (Training)

1: **input:** $\mathcal{D} = \{(\mathcal{X}_1, \mathbf{X}_1), (\mathcal{X}_2, \mathbf{X}_2), \cdots, (\mathcal{X}_d, \mathbf{X}_d)\}$ - training dataset, N - number of layers, T and K - number of sub-layers or sub-iterations

2: **initialize** trainable parameters in $\mathbf{\Theta}$

3: **repeat** for each epoch

(a) **select** (randomly) a batch of samples $\{(\mathcal{X}_i, \mathbf{X}_i)\}$

(b) **predict** output $\mathcal{G}(\mathcal{X}_i, \mathbf{\Theta})$ for each sample $(\mathcal{X}_i, \mathbf{X}_i)$

(c) **compute** loss according to (27) for each sample

(d) **update** learnable parameters via BP

until some training criterion is met

4: **output**: optimized learnable parameters $\mathbf{\Theta}^\star$

Finally, we analyze the computational complexity of the learning algorithm. As the training procedure occupies a very small part of the entire process and can be implemented in the data transmission phase by the BS with powerful computing resources, we focus on the in-service phase. The number of complex multiplications are used to measure the complexity. The complexities of the operations in (18) (including also (26)) and (23)-(25) are given by $\mathcal{O}(2N_{\mathrm{T}}^3 + 4N_{\mathrm{T}}^2 + 2LTN_{\mathrm{T}})$ and $\mathcal{O}\left(4LUTKN_{\mathrm{T}}\right)$, respectively. Hence, the overall computational complexity is $\mathcal{O}\left(2NN_{\mathrm{T}}^3 + 4NN_{\mathrm{T}}^2 + 2NLTN_{\mathrm{T}}\right) + 4NLUTKN_{\mathrm{T}}\big)$. Note that because the core parameters have been optimized, the required number of iterations is very small. Hence, the complexity of the learning-based solution is much smaller than that of an optimization-based one. Note also that although the CRB in (6) is chosen as the objective function in this paper, the algorithms proposed above apply to more general and complex optimization goals as well.

IV. Recursive Beamforming Design

In this section, we propose an efficient recursive approach, whose advantages are, at least, three-fold. First, the objective function value is further decreased, which implies performance improvement in terms of radar sensing. In particular, it always monotonically improves the system performance, and achieves better performance than the previous algorithms, which have been shown to converge to locally optimal solutions. Second, it disperses the computation-intensive task among multiple time-slots, which alleviates the burden of computation resources, improves real-time performance and reduces latency. Third, the recursive algorithms derived often have lower computational complexity, since a vector optimization variable, rather than a matrix variable, is involved in the recursive process.

The recursive method consists of two core operations. The first provides an initial solution, based on which the recursive algorithm can operate. Note that the scale of the problem used to obtain the initial solution should be as small as possible. The second is an efficient algorithm to optimize the precoded signal vector $\mathbf{x}_l$ based on the precoded signal vectors $\mathbf{x}_1, \cdots, \mathbf{x}_{l-1}$. We next elaborate on the details of the recursive approach.

For ease of understanding, we assume that the precoded vector $\mathbf{x}_l$ transmitted in time-slot l is optimized in time-slot $l-1$. The precoded matrix $\mathbf{X}$ can be decomposed as $\mathbf{X} = [\mathbf{X}_{1:l}, \mathbf{X}_{l+1:}]$, where l denotes the index of the current time-slot. Note that for the current time-slot l, the precoded sub-matrix $\mathbf{X}_{l+1:}$ corresponds to the "future waveform" and "future transmitted information symbols". Up to time-slot l, we only need to consider sub-matrix $\mathbf{X}_{1:l}$. Then, the optimization problem can be formulated as

$$\begin{aligned} \min_{\mathbf{X}_{1:l}} \quad & \mathrm{tr}\big((\mathbf{X}_{1:l}\mathbf{X}_{1:l}^{\mathrm{H}})^{-1}\big) \\ \text{s.t.} \quad & \big|\mathrm{Im}(\mathbf{h}_u^{\mathrm{H}}\mathbf{x}_i e^{-j\xi_{u,i}})\big| \le \big(\mathrm{Re}(\mathbf{h}_u^{\mathrm{H}}\mathbf{x}_i e^{-j\xi_{u,i}}) - \gamma_u\big)C_\pi, \\ & \qquad (i = 1, \cdots, l, \forall\, u) \\ & \|\mathbf{x}_i\|^2 \le p, \ (i = 1, \cdots, l). \end{aligned}$$

As a recursive algorithm, when optimizing sub-matrix $\mathbf{X}_{1:l}$, sub-matrix $\mathbf{X}_{1:l-1}$ is already available. Hence, in time-slot $l-1$, the main task is to optimize the precoded vector $\mathbf{x}_l$ given sub-matrix $\mathbf{X}_{1:l-1}$, i.e.,

$$\begin{aligned} \min_{\mathbf{x}_l} \quad & \mathrm{tr}\big((\mathbf{X}_{1:l}\mathbf{X}_{1:l}^{\mathrm{H}})^{-1}\big) \\ \text{s.t.} \quad & \big|\mathrm{Im}(\mathbf{h}_u^{\mathrm{H}}\mathbf{x}_l e^{-j\xi_{u,l}})\big| \le \\ & \qquad \big(\mathrm{Re}(\mathbf{h}_u^{\mathrm{H}}\mathbf{x}_l e^{-j\xi_{u,l}}) - \gamma_u\big)C_\pi, \ (\forall\, u) \\ & \|\mathbf{x}_l\|^2 \le p. \end{aligned} \tag{28}$$

By leveraging the well-known matrix inversion lemma [5], the objective function in problem (28) can be expressed as

$$\begin{aligned} & \big(\mathbf{X}_{1:l}\mathbf{X}_{1:l}^{\mathrm{H}}\big)^{-1} \\ =& \big(\mathbf{X}_{1:l-1}\mathbf{X}_{1:l-1}^{\mathrm{H}} + \mathbf{x}_l\mathbf{x}_l^{\mathrm{H}}\big)^{-1} \\ =& \big(\mathbf{X}_{1:l-1}\mathbf{X}_{1:l-1}^{\mathrm{H}}\big)^{-1} - \\ & \qquad \frac{\big(\mathbf{X}_{1:l-1}\mathbf{X}_{1:l-1}^{\mathrm{H}}\big)^{-1}\mathbf{x}_l\mathbf{x}_l^{\mathrm{H}}\big(\mathbf{X}_{1:l-1}\mathbf{X}_{1:l-1}^{\mathrm{H}}\big)^{-1}}{1 + \mathbf{x}_l^{\mathrm{H}}\big(\mathbf{X}_{1:l-1}\mathbf{X}_{1:l-1}^{\mathrm{H}}\big)^{-1}\mathbf{x}_l}. \end{aligned}$$

[5] $\big(\mathbf{A} + c\mathbf{u}\mathbf{v}^{\mathrm{H}}\big)^{-1} = \mathbf{A}^{-1} - c\mathbf{A}^{-1}\mathbf{u}\mathbf{v}^{\mathrm{H}}\mathbf{A}^{-1}/(1 + c\mathbf{v}^{\mathrm{H}}\mathbf{A}^{-1}\mathbf{u})$.

Let $\mathbf{A}_{l-1} = \big(\mathbf{X}_{1:l-1}\mathbf{X}_{1:l-1}^{\mathrm{H}}\big)^{-1}$. The optimization problem in (28) can be equivalently written as

$$\begin{aligned} \max_{\mathbf{x}_l} \quad & \mathrm{tr}\left(\frac{\mathbf{A}_{l-1}\mathbf{x}_l\mathbf{x}_l^{\mathrm{H}}\mathbf{A}_{l-1}}{1 + \mathbf{x}_l^{\mathrm{H}}\mathbf{A}_{l-1}\mathbf{x}_l}\right) = \frac{\mathbf{x}_l^{\mathrm{H}}\mathbf{A}_{l-1}^2\mathbf{x}_l}{1 + \mathbf{x}_l^{\mathrm{H}}\mathbf{A}_{l-1}\mathbf{x}_l} \\ \text{s.t.} \quad & \big|\mathrm{Im}(\mathbf{h}_u^{\mathrm{H}}\mathbf{x}_l e^{-j\xi_{u,l}})\big| \le \\ & \qquad \big(\mathrm{Re}(\mathbf{h}_u^{\mathrm{H}}\mathbf{x}_l e^{-j\xi_{u,l}}) - \gamma_u\big)C_\pi, \ (\forall\, u) \\ & \|\mathbf{x}_l\|^2 \le p. \end{aligned} \tag{29}$$

Compared to problem (6), whose optimization variable is a matrix, the optimization variable of problem (29) is only a vector. Moreover, the number of constraints in problem (29) is L times smaller than that of problem (6). As a result, the complexity of problem (29) is much smaller than for problem (6). In addition to the low complexity, another potential benefit of the recursive approach is that it disperses the original computation-intensive task among multiple time-slots, which can improve system performance and reduce latency, as it is possible to transmit the first portion of the data without waiting for the entire data matrix to be available. This advantage becomes more pronounced as L increases.

Although problem (29) involves only a vector optimization variable $\mathbf{x}_l$, it cannot be solved directly. Next, we propose an efficient algorithm to address this problem. By introducing a variable t, problem (29) can be equivalently written as

$$\begin{aligned} \max_{\mathbf{x}_l, t} \quad & t \\ \text{s.t.} \quad & t^{-1}\mathbf{x}_l^{\mathrm{H}}\mathbf{A}_{l-1}^2\mathbf{x}_l \ge 1 + \mathbf{x}_l^{\mathrm{H}}\mathbf{A}_{l-1}\mathbf{x}_l \\ & \big|\mathrm{Im}(\mathbf{h}_u^{\mathrm{H}}\mathbf{x}_l e^{-j\xi_{u,l}})\big| \le \\ & \qquad \big(\mathrm{Re}(\mathbf{h}_u^{\mathrm{H}}\mathbf{x}_l e^{-j\xi_{u,l}}) - \gamma_u\big)C_\pi, \ (\forall\, u) \\ & \|\mathbf{x}_l\|^2 \le p. \end{aligned} \tag{30}$$

The successive convex approximation (SCA) technique can be used to solve problem (30), as follows. Let $\mathbf{x}_{l,n}$ and t_n denote the n-th iterations of $\mathbf{x}_l$ and t, respectively. The $(n+1)$-th iterations can be obtained by solving the following convex problem

$$\begin{aligned} \max_{\mathbf{x}_l, t} \quad & t \\ \text{s.t.} \quad & \frac{2\mathrm{Re}\big(\mathbf{x}_{l,n}^{\mathrm{H}}\mathbf{A}_{l-1}^2\mathbf{x}_l\big)}{t_n} - \frac{\mathbf{x}_{l,n}^{\mathrm{H}}\mathbf{A}_{l-1}^2\mathbf{x}_{l,n}}{t_n^2}t \\ & \qquad \ge 1 + \mathbf{x}_l^{\mathrm{H}}\mathbf{A}_{l-1}\mathbf{x}_l \\ & \big|\mathrm{Im}(\mathbf{h}_u^{\mathrm{H}}\mathbf{x}_l e^{-j\xi_{u,l}})\big| \le \\ & \qquad \big(\mathrm{Re}(\mathbf{h}_u^{\mathrm{H}}\mathbf{x}_l e^{-j\xi_{u,l}}) - \gamma_u\big)C_\pi, \ (\forall\, u) \\ & \|\mathbf{x}_l\|^2 \le p. \end{aligned} \tag{31}$$

Algorithm 4: Iterative Algorithm for Problem (29) or (30)

1: **initialize:** optimization variables $\mathbf{x}_{l,0}$ and t_0; let $n = 0$

2: **repeat**

(a) **construct** convex optimization problem (31)

(b) **solve** constructed problem to update $\mathbf{x}_l \Rightarrow \mathbf{x}_{l,n+1}$

(c) **check** convergence criterion and let $n \leftarrow n + 1$

3: **until** some convergence criterion is met

4: **output:** optimal solution $\mathbf{x}_l^\star$

For clarity, the complete iterative procedure to solve problem (29) is summarized in Algorithm 4, which also converges to a stationary point. The optimization variables $\mathbf{x}_l$ and t are initialized first. In step (a) and step (b), a convex problem is constructed and solved to update $\mathbf{x}_l$. The procedure is repeated until some convergence criterion is met.

For completeness, the complete recursive procedure for one communication frame is provided in Algorithm 5. To start the recursive algorithm, an initial solution (i.e., a sub-matrix of $\mathbf{X}$) has to be provided at the beginning. To obtain an initial solution, we can solve the following problem

$$\begin{aligned} \min_{\mathbf{X}\in\mathbb{C}^{N_\mathrm{T}\times K}} \quad & \mathrm{tr}\big((\mathbf{X}\mathbf{X}^\mathrm{H})^{-1}\big) \\ \text{s.t.} \quad & \big|\mathrm{Im}(\mathbf{h}_u^\mathrm{H}\mathbf{x}_l e^{-j\xi_{u,l}})\big| \le \big(\mathrm{Re}(\mathbf{h}_u^\mathrm{H}\mathbf{x}_l e^{-j\xi_{u,l}}) - \gamma_u\big)C_\pi, \\ & \qquad (l=1,\cdots,K, \forall\, u) \\ & \|\mathbf{x}_l\|^2 \le p,\ (l=1,\cdots,K). \end{aligned} \tag{32}$$

Because the size of optimization variable $\mathbf{X}$ in problem (32) is $N_\mathrm{T}\times K$ with $N_\mathrm{T}\le K \ll L$, the computational complexity of problem (32) is small. With the initial solution available, each subsequent precoded signal vector can be obtained via the recursive procedure, which is provided in step 3.

Algorithm 5: Recursive Beamforming Procedure ($L \gg N_\mathrm{T}$)

1: **input:** K - dimension of initial sub-matrix; $\{\mathbf{h}_u\}$ - CSI

2: **initialize:**

(1) **find** an initial sub-matrix $\mathbf{X}_{1:K}$ (and also $\mathbf{A}_K$)

(2) **set** counter $n \leftarrow K$

3: **repeat**

(a) **construct** optimization problem (29) with $l = n+1$

(b) **solve** constructed problem via Algorithm 4 $\Rightarrow$ precoded signal vector $\mathbf{x}_l^\star$ for time-slot l

(c) **update** counter $n \leftarrow n+1$

until $n \ge L$

Finally, we highlight an important property of the proposed recursive algorithm, i.e., the monotonicity of the recursive procedure, which is stated in the following theorem.

Theorem 2. *Under the assumption that initialization problem* (32) *is feasible, the recursive algorithm strictly monotonously decreases the objective function value as the recursive procedure proceeds or index l increases.*

Proof: See Appendix A. ∎

Theorem 2 shows that the proposed recursive algorithm will not degrade system performance. For example, the oscillation or degeneration phenomenon existing widely in many iterative or recursive designs will not occur in our recursive algorithm.

A. Low-Complexity Implementation via Deep Unfolding

To further reduce the complexity, similar to Algorithm 1, we employ the AU techniques to unfold the above algorithms. To unfold Algorithm 5, it is sufficient to unfold Algorithm 4, which boils down to solving problem (29). Note that problem (29) has important fractional structure that should be exploited to achieve better performance. To exploit the structure, we need to design a novel algorithm. For the sake of convenience, problem (29) is rewritten below

$$\begin{aligned} \max_{\mathbf{x}} \quad & \frac{\mathbf{x}^\mathrm{H}\mathbf{A}^2\mathbf{x}}{1+\mathbf{x}^\mathrm{H}\mathbf{A}\mathbf{x}} \\ \text{s.t.} \quad & \big|\mathrm{Im}(\mathbf{h}_u^\mathrm{H}\mathbf{x}e^{-j\xi_u})\big| \le \\ & \qquad \big(\mathrm{Re}(\mathbf{h}_u^\mathrm{H}\mathbf{x}e^{-j\xi_u}) - \gamma_u\big)C_\pi,\ (\forall\, u) \\ & \|\mathbf{x}\|^2 \le p, \end{aligned} \tag{33}$$

For brevity, the index l in problem (29) is omitted in (33).

To exploit the fractional structure of the objective function, the classical Dinkelbach's extended method [52] is chosen to convert problem (33) into a sequence of easier sub-problems indexed by parametric variable ξ_i ($i=1,2,\cdots$), which are successively tackled until some convergence criterion is met. The i-th sub-problem can be expressed by

$$\begin{aligned} \max_{\mathbf{x}} \quad & \mathbf{x}^\mathrm{H}\mathbf{A}^2\mathbf{x} - \xi_i(1+\mathbf{x}^\mathrm{H}\mathbf{A}\mathbf{x}) \\ \text{s.t.} \quad & \big|\mathrm{Im}(\mathbf{h}_u^\mathrm{H}\mathbf{x}e^{-j\xi_u})\big| \le \\ & \qquad \big(\mathrm{Re}(\mathbf{h}_u^\mathrm{H}\mathbf{x}e^{-j\xi_u}) - \gamma_u\big)C_\pi,\ (\forall\, u) \\ & \|\mathbf{x}\|^2 \le p. \end{aligned} \tag{34}$$

By introducing an auxiliary variable $\mathbf{z}$, problem (35) can be equivalently written as

$$\begin{aligned} \min_{\mathbf{x},\mathbf{z}} \quad & \xi_i\mathbf{x}^\mathrm{H}\mathbf{A}\mathbf{x} - \mathbf{x}^\mathrm{H}\mathbf{A}^2\mathbf{x} \\ \text{s.t.} \quad & \big|\mathrm{Im}(\mathbf{h}_u^\mathrm{H}\mathbf{z}e^{-j\xi_u})\big| \le \\ & \qquad \big(\mathrm{Re}(\mathbf{h}_u^\mathrm{H}\mathbf{z}e^{-j\xi_u}) - \gamma_u\big)C_\pi,\ (\forall\, u) \\ & \mathbf{x}=\mathbf{z}, \quad \|\mathbf{x}\|^2 \le p. \end{aligned} \tag{35}$$

Let $\rho>0$ denote the penalty parameter and $\mathbf{y}$ the dual variable for constraint $\mathbf{x}=\mathbf{z}$. Then, the (partial) Lagrangian of problem (35) is given by

$$\begin{aligned} \min_{\mathbf{x},\mathbf{z}} \quad & \xi_i\mathbf{x}^\mathrm{H}\mathbf{A}\mathbf{x} - \mathbf{x}^\mathrm{H}\mathbf{A}^2\mathbf{x} + \frac{\rho}{2}\|\mathbf{x}-\mathbf{z}+\mathbf{y}/\rho\|^2 \\ \text{s.t.} \quad & \big|\mathrm{Im}(\mathbf{h}_u^\mathrm{H}\mathbf{z}e^{-j\xi_u})\big| \le \\ & \qquad \big(\mathrm{Re}(\mathbf{h}_u^\mathrm{H}\mathbf{z}e^{-j\xi_u}) - \gamma_u\big)C_\pi,\ (\forall\, u) \\ & \|\mathbf{x}\|^2 \le p. \end{aligned} \tag{36}$$

Under the assumption that parameter ρ is sufficiently large, problem (36) is convex and can be solved via the alternating optimization method. Specifically, we solve the following two sub-problems in an alternating fashion and update the dual variable.

1) Sub-problem w.r.t. variable $\mathbf{x}$*:* We update variable $\mathbf{x}$ by solving the following problem

$$\begin{aligned} \min_{\mathbf{x}} \quad & \xi_i\mathbf{x}^\mathrm{H}\mathbf{A}\mathbf{x} - \mathbf{x}^\mathrm{H}\mathbf{A}^2\mathbf{x} + \frac{\rho}{2}\|\mathbf{x}-\mathbf{z}+\mathbf{y}/\rho\|^2 \\ \text{s.t.} \quad & \|\mathbf{x}\|^2 \le p. \end{aligned} \tag{37}$$

Since ρ is sufficiently large, problem (37) is strongly convex, and thus the gradient projection method can be invoked to find the optimal solution. The update formula is given by

$$\mathbf{x}_{j+1} = \begin{cases} \mathbf{u}_j & \text{if } \|\mathbf{u}_j\|^2 \le p \\ \sqrt{p}\mathbf{u}_j/\|\mathbf{u}_j\| & \text{otherwise,} \end{cases} \tag{38}$$

where the intermediate variable $\mathbf{u}_j$ is calculated as

$$\mathbf{u}_j = \mathbf{x}_j - \kappa\big(\xi_i\mathbf{A}\mathbf{x}_j - \mathbf{A}^2\mathbf{x}_j + \rho\mathbf{x}_j/2 - \rho\mathbf{z}/2 + \mathbf{y}/2\big). \tag{39}$$

The parameter κ in (39) denotes the step-size.

2) Sub-problem w.r.t. variable $\mathbf{z}$*:* The variable $\mathbf{z}$ is updated by solving the following problem

$$\begin{aligned} \min_{\mathbf{z}} \quad & \|\mathbf{x}-\mathbf{z}+\mathbf{y}/\rho\|^2 \\ \text{s.t.} \quad & \left|\mathrm{Im}(\mathbf{h}_u^{\mathrm{H}}\mathbf{z}e^{-j\xi_u})\right| \le \\ & \left(\mathrm{Re}(\mathbf{h}_u^{\mathrm{H}}\mathbf{z}e^{-j\xi_u})-\gamma_u\right)C_\pi, \ (\forall\, u). \end{aligned} \tag{40}$$

Efficient algorithms have been proposed in Section III to solve this problem, which are omitted here to avoid repetition.

3) Update dual variable $\mathbf{y}$*:* The third step is to update the dual variable $\mathbf{y}$. In the n-th (sub-)iteration, $\mathbf{y}$ is updated as

$$\mathbf{y}_n = \mathbf{y}_{n-1} + \rho(\mathbf{x}_n - \mathbf{z}_n). \tag{41}$$

Similarly, the formula to update parameter ρ is given by

$$\rho_{n+1} = \begin{cases} \beta\rho_n & \|\mathbf{x}_n-\mathbf{z}_n\|^2 > \nu\|\mathbf{x}_{n-1}-\mathbf{z}_{n-1}\|^2 \\ \rho_n & \text{otherwise.} \end{cases} \tag{42}$$

Based on the above discussion, problem (34) can be solved efficiently. The convergence of the iterative algorithm solving problem (34) can be found in [53], [54]. The optimal solution of problem (34) is denoted by $\mathbf{x}_i$. In general, $\mathbf{x}_i$ may not be optimal for problem (33), as parameter ξ_i may not be optimal. But, with $\mathbf{x}_i$ available, the parameter ξ can be updated as

$$\xi_{i+1} = \frac{\mathbf{x}_i^{\mathrm{H}}\mathbf{A}^2\mathbf{x}_i}{1+\mathbf{x}_i^{\mathrm{H}}\mathbf{A}\mathbf{x}_i}. \tag{43}$$

Based on (38) - (43), problem (33) can be efficiently solved, with the complete procedure provided in Algorithm 6, which is a triple-loop iterative algorithm. The outer loop updates the parameter ξ, and the inner double-loop solves problem (35). The convergence criterion can be based on the difference of the objective function values of two successive iterations.

Algorithm 6: Iterative Algorithm for Problem (29)

1: **initialize:** optimization variable $\mathbf{x}_0$ and parameter ξ_0; set counter $i=0$

2: **repeat**

(a) **construct** optimization problem (34)

(b) **repeat** (to solve constructed problem)

(1) **repeat** (to solve primal problem)

1) **update** $\mathbf{x}$ as per (39) and (38)

2) **update** $\mathbf{z}$ by solving problem (40)

until some criterion is met

(2) **update** dual variable $\mathbf{y}$ as per (41)

(3) **update** parameter ρ according to (42)

until some convergence criterion is met

(c) **update** parameter ξ_{i+1} according to (43)

(d) **update** counter $i \leftarrow i+1$

3: **until** some convergence criterion is met

4: **output:** optimal solution $\mathbf{x}^\star$

Next, we further unfold the above iterative algorithm. For sub-problem (37), the update formulas in (38) and (39) are unfolding-friendly by choosing κ as a learnable parameter. As for sub-problem (40), an unfolding-friendly algorithm has been developed in Section III-B. Since all required FP formulas are available, Algorithm 6 has been unfolded. The structure of the unfolded network is depicted in Fig. 4.

The algorithmic network consists of I layers, and each layer consists of 3 sub-layers. The FP formulas are provided in (38), (39) to update $\mathbf{x}$, (23) - (25) to update $\mathbf{z}$, (41) to update $\mathbf{y}$ and (43) to update ξ. The trainable parameters are collected in $\mathbf{\Theta} = \{\kappa_{i,n,j}, \rho_{i,n}, \alpha_{i,n,k} \,|\, i=1,\cdots,I, j=1,\cdots,J, k=1,\cdots,K, n=1,\cdots,N\}$, where $\kappa_{i,n,j}$ is the step-size parameter of the j-th update of the n-th sub-layer within the i-th layer, $\rho_{i,n}$ is the penalty parameter for the n-th sub-layer of the i-th layer, and $\alpha_{i,n,k}$ is the step-size parameter used in (24) and (25) of the k-th update of the n-th sub-layer within the i-th layer. [6]

Algorithm 7: Training of Unfolded Recursive Deep Network

1: **input:** $\mathcal{D} = \{(\mathcal{X}_1, \mathbf{x}_1), (\mathcal{X}_2, \mathbf{x}_2), \cdots, (\mathcal{X}_d, \mathbf{x}_d)\}$ - training dataset, I, N and K - configuration of network

2: **initialize** trainable parameters in $\mathbf{\Theta}$

3: **repeat** for each epoch

(a) **select** (randomly) a batch of samples $\{(\mathcal{X}_i, \mathbf{x}_i)\}$

(b) **predict** output $\mathcal{G}(\mathcal{X}_i, \mathbf{\Theta})$ for each sample $(\mathcal{X}_i, \mathbf{x}_i)$

(c) **compute** loss according to (27) for each sample

(d) **update** learnable parameters via BP

until some training criterion is met

4: **output**: optimized learnable parameters $\mathbf{\Theta}^\star$

The training of the derived network is similar to that of the previous one described in Fig. 3. The details are omitted to avoid repetition. For completeness, the training procedure is summarized in Algorithm 7. Finally, we analyze the computational complexity of the above algorithm. The complexities required to solve problems (37) and (40) within each layer or iteration are $\mathcal{O}(N_{\mathrm{T}}^2+2N_{\mathrm{T}})$ and $\mathcal{O}\big(4KUN_{\mathrm{T}}\big)$, respectively. Hence, the overall complexity is $\mathcal{O}\big((I+1)N_{\mathrm{T}}^3+(IN+L)N_{\mathrm{T}}^2+2INN_{\mathrm{T}}+4INKUN_{\mathrm{T}}\big)$. Note that because the values of key parameters (e.g., N) are very small thanks to deep unfolding and the main iterations within the algorithm can be executed in parallel, the complexity involved is very low in practice.

V. Simulation Results

In this section, simulation results are provided to demonstrate the performance of the proposed algorithms. Without loss of generality, a uniform linear array (ULA) is considered. The distribution of received noise for both communication and radar data is fixed to $\mathcal{CN}(\mathbf{0},\mathbf{I})$. The Rayleigh fading channel model is chosen to evaluate all considered algorithms, i.e., the channel vector of each user u is distributed as $\mathbf{h}_u \sim \mathcal{CN}(\mathbf{0},\mathbf{I})$ [23]. For the iterative algorithms, β and ν take values 1.6 and 0.4, respectively. The initial value of penalty parameter ρ is set to 0.5, which is later updated according to (42). The parameter ε takes value 10^{-4}. The Adam optimizer is chosen to train a deep algorithmic network, with the learning rate 0.002. [7]

[6] Outwardly, the network consists of three levels. However, enjoying the advantages from algorithm unfolding, the network scale can often be small. For example, it works well for the setting $N=8$ and $K=8$.

[7] To promote reproducible research, the dataset and code for generating the simulation results in this paper are made available on the authors' website: https://github.com/Jianjun Zhang-NUAA/JSTSP2024ISAC.

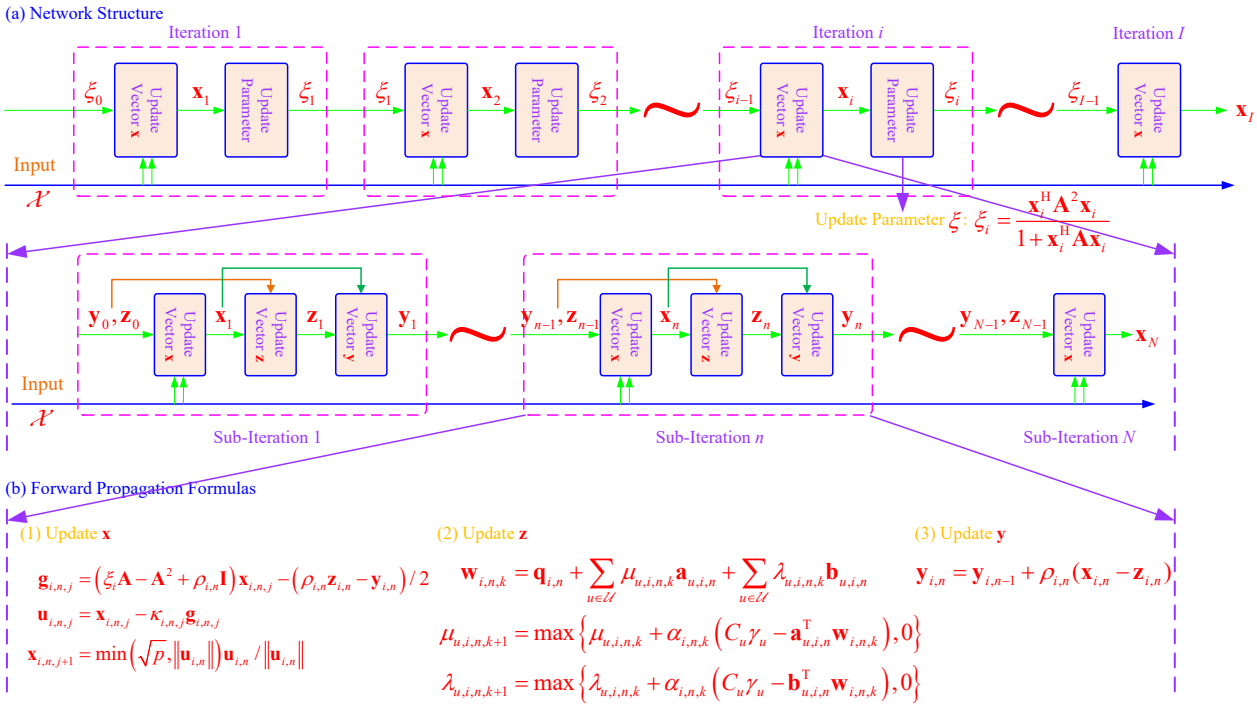

Fig. 4. The network structure and forward propagation formulas of the unfolded deep network derived from the fractional programming based algorithm.

The mean square error (MSE) [8], symbol error rate (SER), normalized mean square error (NMSE) of the beamforming matrix and elapsed time are chosen as performance metrics to evaluate different algorithms. The NMSE is defined as

$$\mathrm{NMSE} = 10\log\frac{\|\hat{\mathbf{X}} - \mathbf{X}^\star\|_{\mathrm{F}}^2}{\|\mathbf{X}^\star\|_{\mathrm{F}}^2}, \tag{44}$$

where $\hat{\mathbf{X}}$ denotes the transmit matrix predicted by algorithmic deep network and $\mathbf{X}^\star$ represents the transmit matrix obtained by optimization-based iterative algorithms in this paper, e.g., Algorithm 1 for the parallelizable design. Similar to [41]–[43], [55], since we concentrate on the reduction of computational complexity, it is appropriate to choose these possible locally optimal solutions as the benchmark or baseline.

To demonstrate the effectiveness of the proposed algorithms, we compare them against the most relevant benchmark in [23], in which the CRB is similarly minimized but using classical block-level precoding (BLP). For brevity, the optimization-based parallelizable algorithm (i.e., Algorithm 1), the learning-based parallelizable algorithm (i.e., Algorithm 3), the optimization-based recursive algorithm (i.e., Algorithm 5) and the learning-based recursive algorithm (i.e., Algorithm 7) are referred to as Optim-Paral-SLP, Learn-Paral-SLP, Optim-Recur-SLP and Learn-Recur-SLP, respectively.

Before evaluating the different algorithms, we first confirm the monotonicity of the proposed recursive approach. As shown in Fig. 5, as the recursive process proceeds (i.e., the index l increases), the MSE decreases strictly and monotonically, which coincides with our theoretical analysis. It is also observed that the MSE decreases fast at the beginning of the recursive process, which implies that good radar sensing performance can be achieved with a small amount of time and computing resources.

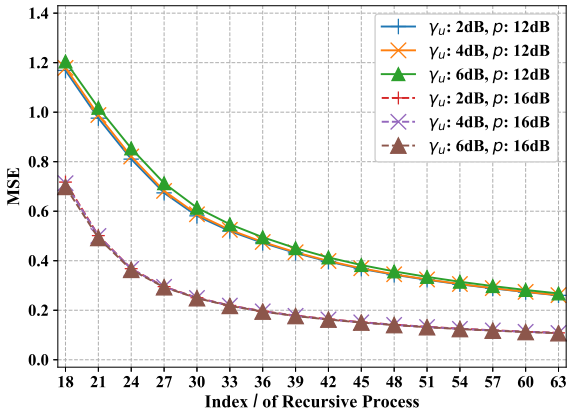

Fig. 5. The monotonicity of the recursive beamforming design (Algorithm 5): $U = 6$, $L = 64$ and $N_{\mathrm{T}} = 16$.

Next, we evaluate different beamforming algorithms from the perspective of MSE and SER. The target estimation MSE of the different algorithms is provided in Fig. 6. Because CI-based SLP can effectively exploit the interference, it is not surprising that the SLP-based algorithms outperform BLP. Interestingly, we see that the two recursive beamforming algorithms are superior to their non-recursive counterparts. In fact,

[8]Note that because of the linear model in (2) and estimating $\mathbf{G}$, $\mathbf{G}$ is absent in the CRB expression. Hence, there is no need to generate matrix $\mathbf{G}$ in the simulations and the simulations also do not depend on how to generate $\mathbf{G}$.

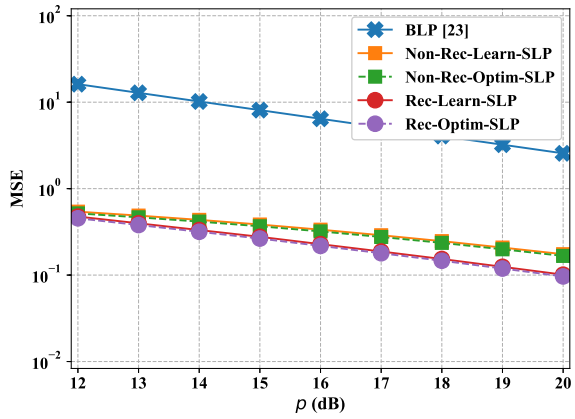

Fig. 6. Target estimation MSE of different beamforming algorithms: $U = 4$, $L = 32$, $N_{\mathrm{T}} = 16$ and $\gamma_u = 8$dB.

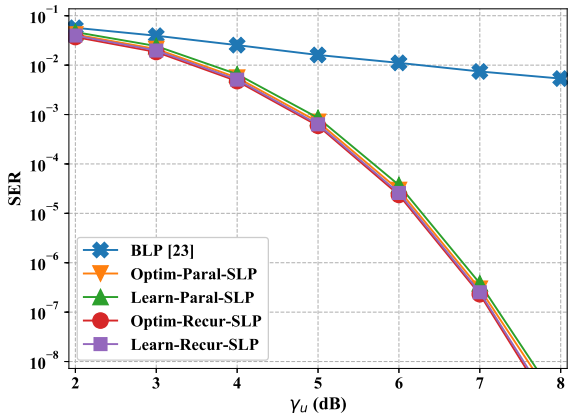

Fig. 8. SER of different beamforming algorithms: $U = 4$, $L = 32$, $N_{\mathrm{T}} = 16$ and $p = 15$dB.

since the objective function of the considered optimization problem is highly nonlinear and non-convex, it is difficult (and even impossible) to find the globally optimal solution. The monotonicity of the recursive algorithms guarantees that the performance metric continually improves, which alleviates the possibly unpredictable influence of the non-convexity of the optimization problem.

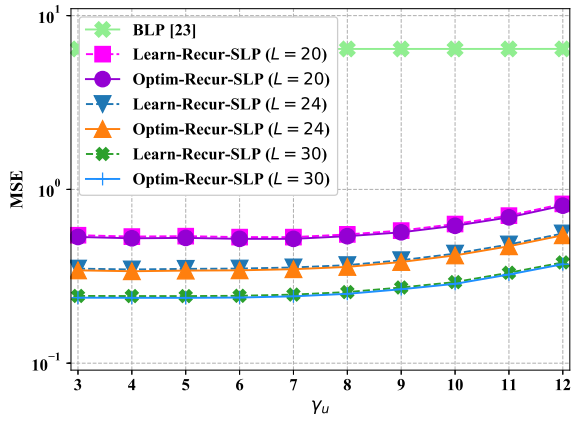

Fig. 7. Target estimation MSE of different beamforming algorithms (varying with γ_u): $U = 4$, $N_{\mathrm{T}} = 16$, $N_{\mathrm{R}} = 24$ and $p = 16$dB.

The performance tradeoff between radar sensing and communication is shown in Fig. 7. The CRB for target estimation becomes higher as the SNR threshold of the UEs increases. Equivalently, as the quality of communication becomes better, the radar sensing performance decreases. Note that although the CRB of the SLP-based algorithms becomes larger as the SNR increases, the CRB remains at a low level, which clearly shows the advantages of the SLP-based design.

We further evaluate different beamforming algorithms from the view of communication. The SER performance of the different algorithms is shown in Fig. 8. It can be observed that the SER performance achieved by the SLP-based algorithms is much better than that of their BLP counterpart. The reason for this is that to exploit the multi-user interference, the CI constraints enforce that the distance between the received signals and the decision boundaries is no less than a predefined value that guarantees a stable SER performance.

It can be observed from Figs. 6 to 8 that the learning-based and the optimization-based algorithms achieve almost the same performance for both radar sensing and communication. However, the complexity of the learning-based solutions is much lower than that of the optimization-based approaches. To better illustrate this point, we take Algorithm 6 based on optimization and its learning-based counterpart in Algorithm 7 as an example and evaluate the NMSE performance of the two in Fig. 9. "Analyzed" indicates that the step-size parameters are obtained via convergence analysis, which guarantees that the iterative algorithm converges.

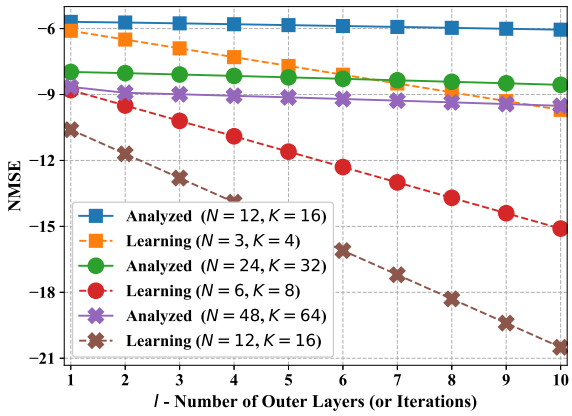

Fig. 9. NMSE of the optimization-based and learning-based beamforming algorithms: $U = 4$, $N_{\mathrm{T}} = 16$, $\gamma_u = 8$dB and $p = 15$dB.

It is seen that compared to the optimization-based iterative design, the learning-based algorithm requires considerably fewer iterations to achieve the same accuracy. In particular, even with only 1/4 of the number of iterations of the optimization-based algorithm, the learning-based approach still performs very well and achieves much lower NMSE. The reason for this is that although the step-size parameters derived via convergence analysis can ensure that an iterative algorithm converges, they are often too conservative, especially for

the early iterations. In fact, for most iterative optimization algorithms, the step-size parameters should decrease gradually as the iteration process proceeds. However, it is difficult to determine such decreasing values via convergence analysis. Fortunately, our learning-based designs can tackle this challenging issue.

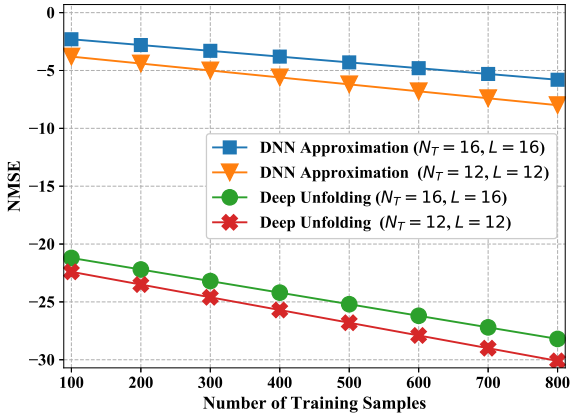

Fig. 10. NMSE of two learning-based beamforming algorithms: $U = 4$, $\gamma_u = 8$dB and $p = 16$dB.

In addition to the low computational complexity, our deep-unfolding based learning algorithms also enjoy the advantages of low training and sample complexity. The NMSE of Algorithm 3 (i.e., a learning-based algorithm) versus the number of samples used for training is shown in Fig. 10. For comparison, the performance of another benchmark is also provided, where a fully-connected deep neural network (DNN) is used to approximate the mapping of Algorithm 1 [55]. It is seen that the proposed learning-based algorithm is superior to the DNN-based approach. The reason for this is as follows. First, since the DNN-based design is driven by "big data", the resultant algorithm is data-hungry. In contrast, since the unfolded algorithm incorporates domain knowledge, the obtained algorithm can greatly reduce the required number of training samples. Moreover, the learnable parameters of our algorithms are mainly scalar step-size parameters, which is a further advantage.

To demonstrate the advantage of our algorithms in terms of computational complexity, the run time of the different beamforming algorithms is compared in Fig. 11. It is observed that our proposed algorithms outperform the baseline algorithm when the number of transmit antennas is greater than 24. The reason for this is two-fold: the baseline algorithm relies on the second-order interior-point method which mainly applies to small-scale optimization problems, while our algorithms are first-order and can be implemented in parallel and/or recursively. It is also observed that the learning-based algorithms run faster than the optimization-based approaches since the learning-based algorithms only consist of simple matrix/vector products and the number of required iterations is very small. The above advantages become more pronounced as the scale of the antenna array or the length of the communication frame increases. Moreover, if the algorithms are implemented on an FPGA platform, which is very good at massively parallel

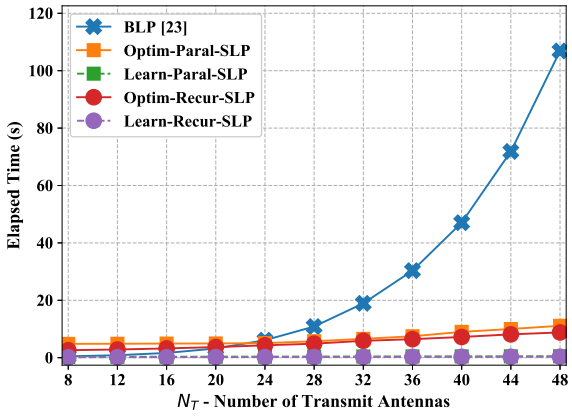

Fig. 11. Running time of different beamforming algorithms: $U = 4$, $\gamma_u = 8$dB and $p = 20$dB.

computing, the potential of parallelizability of our algorithms can be well released and much better real-time performance is expected to be present.

VI. Conclusion

In this paper we proposed efficient low-complexity joint radar sensing and communication beamforming based on the SLP approach to enhance the energy efficiency. First, we proposed highly parallelizable optimization algorithms to reduce the computational complexity. Then, we proposed the idea of recursive design as well as efficient algorithms which can achieve better performance. Finally, to further reduce the complexity, we employed unfolding techniques to design efficient learning-based algorithms for the proposed optimization algorithms. We illustrated the advantages of our algorithms via comprehensive simulation results. The future works include developing efficient parallelizable and recursive algorithms for general DFRC beamforming problems, general deep unfolding methods and efficient DFRC algorithms that exploit features from both communication and radar sensing and investigating DFRC algorithms by choosing specific parameters (like angle and velocity) as sensing metrics and optimizing the CRB.

Appendix A
Proof of Theorem 2

We shall use induction to prove this theorem. Let n denote the induction index, taking values $K, K+1, K+2, \cdots$.

Step 1. For $n = K$, the optimization problem used to find an initial solution is given by

$$\begin{aligned} \min_{\mathbf{X}\in\mathbb{C}^{U\times K}} \quad & \mathrm{tr}\big((\mathbf{X}\mathbf{X}^{\mathrm{H}})^{-1}\big) \\ \text{s.t.} \quad & \big|\mathrm{Im}(\mathbf{h}_u^{\mathrm{H}}\mathbf{x}_l e^{-j\xi_{u,l}})\big| \le \big(\mathrm{Re}(\mathbf{h}_u^{\mathrm{H}}\mathbf{x}_l e^{-j\xi_{u,l}}) - \gamma_u\big)C_\pi, \\ & \quad (l = 1, \cdots, K, \forall\, u) \\ & \|\mathbf{x}_l\|^2 \le p, \ (l = 1, \cdots, K). \end{aligned} \tag{45}$$

According to the assumption of the theorem (i.e., problem (45) is feasible), a solution of the problem, denoted by $\mathbf{X}_K$, satisfies $\mathrm{tr}\big((\mathbf{X}_K\mathbf{X}_K^{\mathrm{H}})^{-1}\big) < \infty$. Combining with the fact

that $\mathbf{X}_K\mathbf{X}_K^{\mathrm{H}} \succeq \mathbf{0}$, we can assert that $\mathbf{X}_K\mathbf{X}_K^{\mathrm{H}} \succ \mathbf{0}$ holds. Hence, $\mathbf{A}_K = (\mathbf{X}_K\mathbf{X}_K^{\mathrm{H}})^{-1}$ is also strictly positive definite, i.e., $\mathbf{A}_K \succ \mathbf{0}$.

To seek the solution for $n = K+1$, the recursive procedure solves the following optimization problem

$$\begin{aligned} \max_{\mathbf{x}_l} \quad & \frac{\mathbf{x}_l^{\mathrm{H}}\mathbf{A}_K^2\mathbf{x}_l}{1+\mathbf{x}_l^{\mathrm{H}}\mathbf{A}_K\mathbf{x}_l} \\ \text{s.t.} \quad & \left|\mathrm{Im}(\mathbf{h}_u^{\mathrm{H}}\mathbf{x}_l e^{-j\xi_{u,l}})\right| \le \\ & \qquad \left(\mathrm{Re}(\mathbf{h}_u^{\mathrm{H}}\mathbf{x}_l e^{-j\xi_{u,l}}) - \gamma_u\right)C_\pi, \ (\forall\, u) \\ & \|\mathbf{x}_l\|^2 \le p. \end{aligned} \tag{46}$$

Since the set of constraints for problem (46) is a proper subset of that of problem (45) and the objective function of problem (46) is well-defined for the entire space $\mathbb{C}^{N_{\mathrm{T}}}$, the feasibility of problem (46) indicates that the feasible set of problem (46), denoted by $\mathcal{F}_l$, is nonempty. Note that $\mathbf{0} \notin \mathcal{F}_l$ holds. Otherwise, the CI constraints are violated.

The solution of problem (46) is denoted by $\mathbf{x}_{K+1}$. Since $\mathbf{A}_K \succ \mathbf{0}$ and $\mathbf{x}_{K+1}\mathbf{x}_{K+1}^{\mathrm{H}} \succeq \mathbf{0}$ hold, we can obtain

$$\begin{aligned} \mathbf{A}_{K+1}^{-1} =& \mathbf{X}_K\mathbf{X}_K^{\mathrm{H}} + \mathbf{x}_{K+1}\mathbf{x}_{K+1}^{\mathrm{H}} \\ =& \mathbf{A}_K^{-1} + \mathbf{x}_{K+1}\mathbf{x}_{K+1}^{\mathrm{H}} \succ \mathbf{0}. \end{aligned}$$

Hence, $\mathbf{A}_{K+1} \succ \mathbf{0}$ holds. Note $\mathbf{A}_K \succ \mathbf{0}$ and $\mathbf{x}_{K+1} \neq 0$ imply that $\mathbf{x}_{K+1}^{\mathrm{H}}\mathbf{A}_K^2\mathbf{x}_{K+1} > 0$ holds, i.e., the objective function must strictly decrease. The above discussion shows that the theorem holds true for $n = K$.

Step 2. It is sufficient to show that the theorem holds as well for $n = N+1$ if it holds for $n = N > K$. Note that the required induction procedure is similar to that in Step 1, and is omitted to avoid repetition. In view of the above discussion and using induction, we have proven the theorem.

REFERENCES

[1] F. Liu, Y. Cui, C. Masouros, J. Xu, T. X. Han, Y. C. Eldar, and S. Buzzi, "Integrated sensing and communications: Toward dual-functional wireless networks for 6g and beyond," *IEEE J. Sel. Areas Commun.*, vol. 40, no. 6, pp. 1728–1767, 2022.

[2] L. Zheng, M. Lops, Y. C. Eldar, and X. Wang, "Radar and communication coexistence: An overview: A review of recent methods," *IEEE Signal Process. Mag.*, vol. 36, no. 5, pp. 85–99, 2019.

[3] F. Liu, C. Masouros, A. P. Petropulu, H. Griffiths, and L. Hanzo, "Joint radar and communication design: Applications, state-of-the-art, and the road ahead," *IEEE Trans. Commun.*, vol. 68, no. 6, pp. 3834–3862, 2020.

[4] J. A. Zhang, F. Liu, C. Masouros, R. W. Heath, Z. Feng, L. Zheng, and A. Petropulu, "An overview of signal processing techniques for joint communication and radar sensing," *IEEE J. Sel. Topics Signal Process.*, vol. 15, no. 6, pp. 1295–1315, 2021.

[5] Y. Cui, F. Liu, X. Jing, and J. Mu, "Integrating sensing and communications for ubiquitous IoT: Applications, trends, and challenges," *IEEE Netw.*, vol. 35, no. 5, pp. 158–167, 2021.

[6] F. Liu, C. Masouros, A. Li, H. Sun, and L. Hanzo, "MU-MIMO communications with MIMO radar: From co-existence to joint transmission," *IEEE Trans. Wireless Commun.*, vol. 17, no. 4, pp. 2755–2770, 2018.

[7] A. Zhang, M. L. Rahman, X. Huang, Y. J. Guo, S. Chen, and R. W. Heath, "Perceptive mobile networks: Cellular networks with radio vision via joint communication and radar sensing," *IEEE Veh. Technol. Mag.*, vol. 16, no. 2, pp. 20–30, 2021.

[8] A. Ali, N. Gonzalez-Prelcic, R. W. Heath, and A. Ghosh, "Leveraging sensing at the infrastructure for mmWave communication," *IEEE Commun. Mag.*, vol. 58, no. 7, pp. 84–89, 2020.

[9] P. Kumari, S. A. Vorobyov, and R. W. Heath, "Adaptive virtual waveform design for millimeter-wave joint communicationcradar," *IEEE Trans. Signal Process.*, vol. 68, pp. 715–730, 2020.

[10] G. Duggal, S. Vishwakarma, K. V. Mishra, and S. S. Ram, "Doppler-resilient 802.11ad-based ultrashort range automotive joint radar-communications system," *IEEE Trans. Aerosp. Electron. Syst.*, vol. 56, no. 5, pp. 4035–4048, 2020.

[11] A. Hassanien, M. G. Amin, E. Aboutanios, and B. Himed, "Dual-function radar communication systems: A solution to the spectrum congestion problem," *IEEE Signal Process. Mag.*, vol. 36, no. 5, pp. 115–126, 2019.

[12] K. Wu, J. A. Zhang, X. Huang, Y. J. Guo, and R. W. Heath, "Waveform design and accurate channel estimation for frequency-hopping MIMO radar-based communications," *IEEE Trans. Commun.*, vol. 69, no. 2, pp. 1244–1258, 2021.

[13] T. Huang, N. Shlezinger, X. Xu, Y. Liu, and Y. C. Eldar, "MAJoRCom: A dual-function radar communication system using index modulation," *IEEE Trans. Signal Process.*, vol. 68, pp. 3423–3438, 2020.

[14] F. Liu, L. Zhou, C. Masouros, A. Li, W. Luo, and A. Petropulu, "Toward dual-functional radar-communication systems: Optimal waveform design," *IEEE Trans. Signal Process.*, vol. 66, no. 16, pp. 4264–4279, 2018.

[15] X. Liu, T. Huang, N. Shlezinger, Y. Liu, J. Zhou, and Y. C. Eldar, "Joint transmit beamforming for multiuser MIMO communications and MIMO radar," *IEEE Trans. Signal Process.*, vol. 68, pp. 3929–3944, 2020.

[16] Z. Cheng, S. Shi, Z. He, and B. Liao, "Transmit sequence design for dual-function radar-communication system with one-bit DACs," *IEEE Trans. Wireless Commun.*, vol. 20, no. 9, pp. 5846–5860, 2021.

[17] N. T. Nguyen, L. V. Nguyen, N. Shlezinger, Y. C. Eldar, A. L. Swindlehurst, and M. Juntti, "Joint communications and sensing hybrid beamforming design via deep unfolding," *arXiv:2307.04376*, 2023.

[18] J. Qian, M. Lops, L. Zheng, X. Wang, and Z. He, "Joint system design for coexistence of MIMO radar and MIMO communication," *IEEE Trans. Signal Process.*, vol. 66, no. 13, pp. 3504–3519, 2018.

[19] N. Su, F. Liu, and C. Masouros, "Secure radar-communication systems with malicious targets: Integrating radar, communications and jamming functionalities," *IEEE Trans. Wireless Commun.*, vol. 20, no. 1, pp. 83–95, 2021.

[20] X. Yuan, Z. Feng, J. A. Zhang, W. Ni, R. P. Liu, Z. Wei, and C. Xu, "Spatio-temporal power optimization for MIMO joint communication and radio sensing systems with training overhead," *IEEE Trans. Veh. Technol.*, vol. 70, no. 1, pp. 514–528, 2021.

[21] Y. Liu, G. Liao, J. Xu, Z. Yang, and Y. Zhang, "Adaptive OFDM integrated radar and communications waveform design based on information theory," *IEEE Commun. Lett.*, vol. 21, no. 10, pp. 2174–2177, 2017.

[22] R. Niu, R. S. Blum, P. K. Varshney, and A. L. Drozd, "Target localization and tracking in noncoherent multiple-input multiple-output radar systems," *IEEE Trans. Aerosp. Electron. Syst.*, vol. 48, no. 2, pp. 1466–1489, 2012.

[23] F. Liu, Y.-F. Liu, A. Li, C. Masouros, and Y. C. Eldar, "Cramer-Rao bound optimization for joint radar-communication beamforming," *IEEE Trans. Signal Process.*, vol. 70, pp. 240–253, 2022.

[24] M. D. Larsen, A. L. Swindlehurst, and T. Svantesson, "Performance bounds for MIMO-OFDM channel estimation," *IEEE Trans. Signal Process.*, vol. 57, no. 5, pp. 1901–1916, 2009.

[25] A. M. Elbir, K. V. Mishra, and S. Chatzinotas, "Terahertz-band joint ultra-massive MIMO radar-communications: Model-based and model-free hybrid beamforming," *IEEE J. Sel. Topics Signal Process.*, vol. 15, no. 6, pp. 1468–1483, 2021.

[26] Q. Liu, Y. Zhu, M. Li, R. Liu, Y. Liu, and Z. Lu, "DRL-based secrecy rate optimization for RIS-assisted secure isac systems," *IEEE Trans. Veh. Technol.*, vol. 72, no. 12, pp. 16 871–16 875, 2023.

[27] X. Gao, L. Dai, S. Han, C. I, and R. W. Heath, "Energy-efficient hybrid analog and digital precoding for mmwave mimo systems with large antenna arrays," *IEEE J. Sel. Areas Commun.*, vol. 34, no. 4, pp. 998–1009, 2016.

[28] X. Yu, J. Shen, J. Zhang, and K. B. Letaief, "Alternating minimization algorithms for hybrid precoding in millimeter wave MIMO systems," *IEEE J. Sel. Topics Signal Process.*, vol. 10, no. 3, pp. 485–500, 2016.

[29] J. Zhang, Y. Huang, J. Wang, and L. Yang, "Hybrid precoding for wideband millimeter-wave systems with finite resolution phase shifters," *IEEE Trans. Veh. Technol.*, vol. 67, no. 11, pp. 11 285–11 290, Nov 2018.

[30] C. Masouros and E. Alsusa, "Dynamic linear precoding for the exploitation of known interference in MIMO broadcast systems," *IEEE Trans. Wireless Commun.*, vol. 8, no. 3, pp. 1396–1404, 2009.

[31] C. Masouros, "Correlation rotation linear precoding for MIMO broadcast communications," *IEEE Trans. Signal Process.*, vol. 59, no. 1, pp. 252–262, 2011.

[32] C. Masouros and T. Ratnarajah, "Interference as a source of green signal power in cognitive relay assisted co-existing MIMO wireless transmissions," *IEEE Trans. Commun.*, vol. 60, no. 2, pp. 525–536, 2012.

[33] C. Masouros, T. Ratnarajah, M. Sellathurai, C. B. Papadias, and A. K. Shukla, "Known interference in the cellular downlink: a performance limiting factor or a source of green signal power?" *IEEE Commun. Mag.*, vol. 51, no. 10, pp. 162–171, 2013.

[34] C. Masouros, M. Sellathurai, and T. Ratnarajah, "Vector perturbation based on symbol scaling for limited feedback MISO downlinks," *IEEE Trans. Signal Process.*, vol. 62, no. 3, pp. 562–571, 2014.

[35] A. Li, D. Spano, J. Krivochiza, S. Domouchtsidis, C. G. Tsinos, C. Masouros, S. Chatzinotas, Y. Li, B. Vucetic, and B. Ottersten, "A tutorial on interference exploitation via symbol-level precoding: Overview, state-of-the-art and future directions," *IEEE Communications Surveys Tutorials*, vol. 22, no. 2, pp. 796–839, 2020.

[36] C. Masouros and G. Zheng, "Exploiting known interference as green signal power for downlink beamforming optimization," *IEEE Trans. Signal Process.*, vol. 63, no. 14, pp. 3628–3640, 2015.

[37] F. Liu, C. Masouros, A. Li, T. Ratnarajah, and J. Zhou, "MIMO radar and cellular coexistence: A power-efficient approach enabled by interference exploitation," *IEEE Trans. Signal Process.*, vol. 66, no. 14, pp. 3681–3695, 2018.

[38] R. Liu, M. Li, Q. Liu, and A. L. Swindlehurst, "Dual-functional radar-communication waveform design: A symbol-level precoding approach," *IEEE J. Sel. Topics Signal Process.*, vol. 15, no. 6, pp. 1316–1331, 2021.

[39] ——, "Joint waveform and filter designs for stap-slp-based MIMO-DFRC systems," *IEEE J. Sel. Areas Commun.*, vol. 40, no. 6, pp. 1918–1931, 2022.

[40] L. Wu, B. Wang, Z. Cheng, B. S. M. R, and B. Ottersten, "Joint symbol-level precoding and sub-block-level RIS design for dual-function radar-communications," in *2023 ICASSP*, 2023, pp. 1–5.

[41] K. Metwaly, J. Kweon, K. Alhujaili, M. Greco, F. Gini, and V. Monga, "Interpretable, unrolled deep radar beampattern design," in *2023 IEEE International Conference on Acoustics, Speech and Signal Processing (ICASSP)*, 2023, pp. 1–5.

[42] B. Kang, J. Kweon, M. Rangaswamy, and V. Monga, "Deep learning for radar waveform design: Retrospectives and the road ahead," in *2023 IEEE International Radar Conference (RADAR)*, 2023, pp. 1–6.

[43] S. Khobahi, A. Bose, and M. Soltanalian, "Deep radar waveform design for efficient automotive radar sensing," in *2020 IEEE 11th Sensor Array and Multichannel Signal Processing Workshop (SAM)*, 2020, pp. 1–5.

[44] E. Tohidi, M. Coutino, S. P. Chepuri, H. Behroozi, M. M. Nayebi, and G. Leus, "Sparse antenna and pulse placement for colocated mimo radar," *IEEE Trans. Signal Process.*, vol. 67, no. 3, pp. 579–593, 2019.

[45] S. M. Kay, *Fundamentals of Statistical Signal Processing Volume I: Estimation Theory*. Englewood Cliffs, NJ, USA: Prentice Hall, 1998.

[46] J. R. Magnus and H. Neudecker, *Matrix Differential Calculus with Applications in Statistics and Econometrics*, 3rd ed. Wiley, 2019.

[47] D. P. Bertsekas, *Nonlinear Programming*, 2nd ed. Athena Scientific, 1999.

[48] Z. Lin, H. Li, and C. Fang, *Accelerated Optimization for Machine Learning: First-Order Algorithms*. Springer, 2020.

[49] A. Ruszczynski, *Nonlinear Optimization*. Princeton University Press, 2011.

[50] Y. Sun, P. Babu, and D. P. Palomar, "Majorization-minimization algorithms in signal processing, communications, and machine learning," *IEEE Trans. Signal Process.*, vol. 65, no. 3, pp. 794–816, 2017.

[51] V. Monga, Y. Li, and Y. C. Eldar, "Algorithm unrolling: Interpretable, efficient deep learning for signal and image processing," *IEEE Signal Process. Mag.*, vol. 38, no. 2, pp. 18–44, 2021.

[52] R. G. Rddenas, M. L. Ldpez, and D. Verastegui, "Extensions of Dinkelbach's algorithm for solving non-linear fractional programming problems," *Top*, vol. 7, no. 1, pp. 33–70, 1999.

[53] Q. Shi and M. Hong, "Penalty dual decomposition method for nonsmooth nonconvex optimization - Part I: Algorithms and convergence analysis," *IEEE Trans. Signal Process.*, vol. 68, pp. 4108–4122, 2020.

[54] Q. Shi, M. Hong, X. Fu, and T.-H. Chang, "Penalty dual decomposition method for nonsmooth nonconvex optimization - Part II: Applications," *IEEE Trans. Signal Process.*, vol. 68, pp. 4242–4257, 2020.

[55] H. Sun, X. Chen, Q. Shi, M. Hong, X. Fu, and N. D. Sidiropoulos, "Learning to optimize: Training deep neural networks for interference management," *IEEE Trans. Signal Process.*, vol. 66, no. 20, pp. 5438–5453, 2018.

Responses to Reviewers' Comments for Manuscript J-STSP-SPISC-00082-2023.R1

Low-Complexity Joint Radar-Communication Beamforming: From Optimization to Deep Unfolding

Jianjun Zhang, Christos Masouros, Fan Liu, Yongming Huang and A. Lee Swindlehurst

August 13, 2024

Dear Editor,

We would like to thank you for handling the review process of our paper. We are also indebted to you and the reviewers for the helpful comments. According to your suggestions and comments, we have updated the previous manuscript and submitted a revised version. We summarise the most significant revisions in our paper as follows:

- In response to Comment 2 from you and Comment 10 from Reviewer 2, we have read more references and confirmed the effectiveness of our algorithm and its convergence.
- In response to Comment 3 from you, Comments 6 and 8 from Reviewer 2 and Comment 4 from Reviewer 3, we have explained in detail the necessity and rationality of using the CRB of $\mathbf{G}$ as the optimization goal and introduced the problem formulated more clearly and naturally.
- In response to Comment 4 from you, Comment 11 from Reviewer 2 and Comments 1 and 5 from Reviewer 3, we have perfected our algorithms or statements and made them more rigorous. We have also explained and clarified the properties of the solutions obtained from our algorithms, as per Comments 2 and 3 from Reviewer 3.
- In response to Comment 4 from you and Comment 1 from Reviewer 1, we have cited more relevant papers and included them in the references in the revised manuscript.
- We have explained and clarified the motivation and contributions of our paper in response to Comments 1 and 2 from Reviewer 2. We have also added more discussions and clarifications in response to other comments of Reviewer 2.

In this revision, all of the comments raised by the reviewers have been addressed. To enhance legibility of this response letter, the reviewers' comments are typeset in *italic font* and our responses are written in plain font.

Yours Sincerely,

Jianjun Zhang, Christos Masouros, Fan Liu, Yongming Huang and A. Lee Swindlehurst

IEEE Journal of Selected Topics in Signal Processing
Paper ID: J-STSP-SPISC-00082-2023.R1
Authors' Response to Editor

We would like to thank you for your insightful suggestions and comments, which have helped us improve the quality of our paper. We have revised our paper incorporating all your suggestions and comments.

Comment 1:

1. While I invite you to respond to the reviewers on the various queries, many of them seeking clarifications or results, two broad areas need additional investigation. These relate to the optimization per se and to the radar modelling. I have taken the liberty of adding a few of my comments for authors' consideration on these aspects:

Response:

Thank you very much for your constructive comments and helpful suggestions.

Comment 2:

2. 1) Optimization Aspects: As pointed out by Reviewer 3, comment 9, the method proposed uses the first order derivative to approximate the objective and, in that sense, the original problem is not solved using the gradient projection method. The authors should revisit this claim. Further, it should be noted that since the derivative of the inverse is being considered, one would need to be careful of discontinuities introduced by potential rank reductions in X. It would be good for the authors to keep track of the condition number as well and mention the validity of the approximation.

Response:

We are very grateful to you for your insightful comment and helpful suggestions. We would like to clarify that although the first-order derivative is utilized to approximate the objective, the problem considered in our paper is indeed solved by the gradient projection method, motivated by speeding up the convergence rate. We would like to elaborate on this point from two aspects: 1) the gradient projection method can solve a kind of non-convex problems; and 2) our problem is really solved by the gradient projection method. By the way, we would like to correct the statement of Reviewer 2 that "Anyhow, the gradient projection method is only valid for convex function".

1) Although many textbooks take a convex optimization problem (often a quadratic programming) as an example to elaborate on the principle of the gradient projection method, it is, in fact, an effective method to solve a special kind of nonlinear optimization problems (Section 2.3 of [R1]), whose constraint set $\mathcal{C}$ is closed and convex and objective $f(\boldsymbol{x})$ is continuously differentiable, i.e.,

$$\begin{aligned} \min_{\boldsymbol{x}} \quad & f(\boldsymbol{x}) \\ \text{s.t.} \quad & \boldsymbol{x} \in \mathcal{C}. \end{aligned} \tag{1}$$

[R1] D. P. Bertsekas, *Nonlinear Programming*, 2nd ed. Athena Scientific, 1999.

Note that if the function $f(\boldsymbol{x})$ is convex, the optimization problem is a convex problem. But it is a non-convex problem if $f(\boldsymbol{x})$ is not convex. In Section 2.3 of [R1], the author takes problem (1) as an example to elaborate on the principle and usage of gradient projection method and also provides the convergence analysis. By the way, we would like to mention that the assumption or requirement on the objective function $f(\cdot)$ is continuously differentiable, rather than convex, continuously convex differentiable or other conditions with convexity assumption.

2) We would like to explain that besides the trick of first-order approximation, a quadratic penalty term is also incorporated into the objection function, which therefore makes the gradient projection method applicable. [1] For clarity, the problem solved in this paper is rewritten below:

$$\begin{aligned} \min_{\mathbf{X}} \quad & -\mathrm{Re}\big(\mathrm{tr}((\mathbf{X}_n\mathbf{X}_n^{\mathrm{H}})^{-2}\mathbf{X}_n\mathbf{X}^{\mathrm{H}})\big) + \frac{\rho_n}{2}\|\mathbf{X}-\mathbf{X}_n\|_{\mathrm{F}}^2 \\ \text{s.t.} \quad & \big|\mathrm{Im}(\mathbf{h}_u^{\mathrm{H}}\mathbf{x}_l e^{-j\xi_{u,l}})\big| \le \big(\mathrm{Re}(\mathbf{h}_u^{\mathrm{H}}\mathbf{x}_l e^{-j\xi_{u,l}}) - \gamma_u\big)C_\pi, \ (\forall\, u,l) \\ & \|\mathbf{x}_l\|^2 \le p, \ (\forall\, l), \end{aligned} \tag{2}$$

which can be equivalently written as

$$\begin{aligned} \min_{\mathbf{X}} \quad & \|\mathbf{X}-\mathbf{X}_n-\mathbf{C}_n/\rho_n\|_{\mathrm{F}}^2 \\ \text{s.t.} \quad & \big|\mathrm{Im}(\mathbf{h}_u^{\mathrm{H}}\mathbf{x}_l e^{-j\xi_{u,l}})\big| \le \big(\mathrm{Re}(\mathbf{h}_u^{\mathrm{H}}\mathbf{x}_l e^{-j\xi_{u,l}}) - \gamma_u\big)C_\pi, \ (\forall\, u,l) \\ & \|\mathbf{x}_l\|^2 \le p, \ (\forall\, l). \end{aligned} \tag{3}$$

For brevity, the feasible set of problem (3) is denoted by $\mathcal{F}$ (which is a closed convex set), i.e.,

$$\mathcal{F} = \big\{\mathbf{X}\,\big|\,\|\mathbf{x}_l\|^2 \le p, (\forall\, l), \quad \big|\mathrm{Im}(\mathbf{h}_u^{\mathrm{H}}\mathbf{x}_l e^{-j\xi_{u,l}})\big| \le \big(\mathrm{Re}(\mathbf{h}_u^{\mathrm{H}}\mathbf{x}_l e^{-j\xi_{u,l}}) - \gamma_u\big)C_\pi, (\forall\, u,l)\big\}.$$

According to the definition of projection in the Euclidean space [2], the solution of problem (3), as well as the iteration format solving problem (7) in our paper, can be expressed as:

$$\mathbf{X}_{n+1} = \mathrm{Proj}_{\mathcal{F}}(\mathbf{X}_n + \mathbf{C}_n/\rho_n). \tag{4}$$

The convergence can be obtained immediately according to Proposition 2.3.3 of [R1].

It is true that the phenomenon of rank-defect may occur. But fortunately, inspired by you, we can monitor or detect it by tracking or checking the condition number or the objective function value. Maybe thanks to the CI constraints and the quadratic term, which greatly limit the direction and its variation of variable $\mathbf{X}$, we have not yet observed the phenomenon of rank-defect in the simulation experiment till now, which, to some extent, confirms the validity of our approximation.

Following your suggestion, we have updated our manuscript as follows:

[1] We would like to mention that the derived iterative algorithm still converges, even if the quadratic term is absent. In fact, the derived algorithm becomes the conditional gradient algorithm in this case, whose convergence rate is often (much) lower than that of the gradient projection based counterpart.

[2] The projection of a point $\boldsymbol{x}$ on a closed convex set $\mathcal{C}$, denoted by $\boldsymbol{x}^\star$, is defined as $\boldsymbol{x}^\star \triangleq \mathrm{Proj}_{\mathcal{C}}(\boldsymbol{x}) = \arg\min_{\boldsymbol{y}\in\mathcal{C}} ||\boldsymbol{y}-\boldsymbol{x}||^2$ (Appendix B of [R1]).

The 1-st Paragraph of Left Column of Page 5:

... Note also that theoretically the matrix variable $\mathbf{X}$ may be rank-deficient due to the first-order approximation. If necessary, the phenomenon of rank-defect can be detected or monitored via checking or tracking the condition number or objective function value. But in practice, this phenomenon has not yet been observed, maybe thanks to the CI constraints and quadratic term, which shows its safety and validity.

Proof of Theorem 1 (Page 5):

For brevity, the feasible set of problem (12), which is closed and convex, is denoted by $\mathcal{F}$, i.e.,

$$\mathcal{F} = \big\{\mathbf{X} \,\big|\, \|\mathbf{x}_l\|^2 \le p, (\forall\, l), \quad \big|\mathrm{Im}(\mathbf{h}_u^{\mathrm{H}}\mathbf{x}_l e^{-j\xi_{u,l}})\big| \le \big(\mathrm{Re}(\mathbf{h}_u^{\mathrm{H}}\mathbf{x}_l e^{-j\xi_{u,l}}) - \gamma_u\big)C_\pi, (\forall\, u, l)\big\}.$$

Then, problem (12) can be equivalently written as

$$\begin{aligned} \min_{\mathbf{X}} \quad & \|\mathbf{X} - \mathbf{X}_n - \mathbf{C}_n/\rho_n\|_{\mathrm{F}}^2 \\ \text{s.t.} \quad & \mathbf{X} \in \mathcal{F}. \end{aligned} \tag{5}$$

According to the definition of projection in a Euclidean space [a], the optimal solution of problem (5), denoted by $\mathbf{X}_{n+1}$, can be compactly expressed as

$$\mathbf{X}_{n+1} = \mathrm{Proj}_{\mathcal{F}}(\mathbf{X}_n + \mathbf{C}_n/\rho_n). \tag{6}$$

Under some step-size criterion or rule [b], the convergence of the iteration in (6) can be obtained immediately, e.g., by invoking Proposition 2.3.3 in [47].

[a] The projection of a point $\boldsymbol{x}$ on a closed convex set $\mathcal{C}$, denoted by $\boldsymbol{x}^\star$, is defined as $\boldsymbol{x}^\star \triangleq \mathrm{Proj}_{\mathcal{C}}(\boldsymbol{x}) = \arg\min_{\boldsymbol{y}\in\mathcal{C}} ||\boldsymbol{y} - \boldsymbol{x}||^2$ (Appendix B of [47]).

[b] Note that although the expression in (6) is brief and compact, a closed-form solution is still unavailable. Hence, an iterative algorithm has to be invoked to tackle it, which involves the step-size parameter. Various step-size rules have been available, such as the Armijo or Goldstein rules [47].

Comment 3:

3. 2) Modelling: Two of the reviewers have raised queries on the use of the matrix $\mathbf{G}$*. Clearly,* $\mathbf{G}$ *makes the derivation tractable, however, it increases the "parameters estimated". For two static targets in a monostatic radar setting, one would have 4 parameters (RCS + AoA), but* $\mathbf{G}$ *would involve the dimension of the steering vector; could this be a reason for the higher dimensionalities involved? Further, the derived CRB is not that for the radar parameters and is unclear how to obtain CRB for those parameters from the proposed derivation. Indeed, improvements in estimation can be obtained, but that cannot be quantified. The authors need to motivate their approach better or redefine so as to make the inclusion of* $\mathbf{G}$ *natural to the problem.*

Response:

We very much appreciate your insightful and helpful comments. We agree with you that compared

with the estimation of specific parameters (e.g., velocity, distance or angle of arrival), the dimensionality of $\mathbf{G}$ to be estimated is much higher. But fortunately, matrix $\mathbf{G}$ has very strong structural features (e.g., it is the sum of products of two array response vectors) and the elements in $\mathbf{G}$ are not independent, which can be exploited when further estimating the parameters of interest.

[R1] E. Tohidi, M. Coutino, S. P. Chepuri, H. Behroozi, M. M. Nayebi, and G. Leus, "Sparse antenna and pulse placement for colocated mimo radar," *IEEE Trans. Signal Process.*, vol. 67, no. 3, pp. 579–593, 2019.

We would like to explain that different from [R1] provided in the next comment, where the CRB for direction cosine and radial velocity is derived and chosen as the measure to optimize antenna and pulse placement, we choose to estimate $\mathbf{G}$ and improve its quality for the following reasons:

- First and foremost, the BS often has no prior knowledge about the number of scatterers or targets and different applications or tasks often have different estimation goals. Therefore, it is difficult (and even impossible) to derive a general analytic expression of CRB. [3]
- To derive an analytic expression of CRB for some specific parameters of interest (e.g., velocity and distance), the techniques used by the receiver often have to be taken into account, which inevitably complicates the design of transmit waveform and limits its application scope.
- If $\mathbf{G}$ can be estimated efficiently, sophisticated array signal processing algorithms can be later invoked to extract the information of interest from $\mathbf{G}$. As an example, parameters like angles and reflection coefficients can be extracted from $\mathbf{G}$ via the MUSIC and APES algorithms.

Because of the reasons above, similar to [R2], we decouple or decompose a practical estimation task into two sub-tasks, i.e., the upstream task and downstream task. The upstream task considered in our paper is in charge of designing transmit waveform, while the downstream task is responsible for estimating the practical parameters of interest. Moreover, if necessary, the receiver techniques should be taken into consideration in the downstream task to improve the estimation quality.

[R2] F. Liu, Y.-F. Liu, A. Li, C. Masouros, and Y. C. Eldar, "Cramer-Rao bound optimization for joint radar-communication beamforming," *IEEE Trans. Signal Process.*, vol. 70, pp. 240–253, 2022.

Finally, we would like to elaborate on the upstream task in our paper. Clearly, an important goal is to design the transmit waveform matrix $\mathbf{X}$, so as to make the estimation of $\mathbf{G}$ accurate and simple. Given the linear received signal model $\mathbf{Y}_{\mathrm{R}} = \mathbf{G}\mathbf{X} + \mathbf{Z}_{\mathrm{R}}$, an estimator of $\mathbf{G}$, which is calculated easily, can be obtained via the pseudo-inverse method and is given by $\hat{\mathbf{G}} = \mathbf{Y}_{\mathrm{R}}\mathbf{X}^{\mathrm{H}}\big(\mathbf{X}\mathbf{X}^{\mathrm{H}}\big)^{-1}$. It can be verified that the estimator $\hat{\mathbf{G}}$ is unbiased, i.e., $\mathbb{E}(\hat{\mathbf{G}}) = \mathbf{G}$, with the mean square error (MSE) $N_{\mathrm{R}}\sigma_{\mathrm{R}}^2\mathrm{tr}\big(\mathbf{X}\mathbf{X}^{\mathrm{H}}\big)^{-1}$. Via some calculations, we can verify that the CRB and the MSE of $\hat{\mathbf{G}}$ coincide. This shows that the estimator is also, in a certain sense, optimal, as the MSE attains the CRB. Hence, it is natural to optimize transmit waveform $\mathbf{X}$ by minimizing the CRB or MSE of $\mathbf{G}$.

[3] To tackle this issue, the two-target case is considered in [R1] and the CRB expression for direction cosine and radial velocity is derived.

Based on the above discussion, we hope that you could understand why an explicit expression about $\mathbf{G}$ is absent in our approach and could also acknowledge the rationality of our problem formulation. Following your suggestion, we have updated our manuscript as follows:

The Last Paragraph of Page 3:

In many cases, the Cramér-Rao bound (CRB) of specific parameters of interest is chosen as the performance metric to characterize the sensing performance, e.g., the direction cosine and radial velocity are considered in [44]. But similar to [23], the CRB of $\mathbf{G}$, instead of specific parameters, is chosen as the performance metric and optimization goal here. Essentially, we decouple or decompose a practical estimation task into two sub-tasks, i.e., the upstream task and downstream task. The upstream task is in charge of designing the transmit waveform $\mathbf{X}$, while the downstream task is responsible for estimating the specific parameters of interest. Moreover, if necessary, the receiver techniques should also be taken into account in the downstream task to improve the estimation quality.

The 2-nd Paragraph of Page 4:

The reasons to decompose a practical estimation task into two sub-tasks are as follows. First and foremost, the BS often has no prior knowledge about the number of scatterers or targets and different applications often have different estimation objectives. Second, to derive an analytic expression of CRB for specific parameters, the techniques used by the receiver often have to be taken into account, which complicates the design of $\mathbf{X}$ and limits the application scope. Finally, if $\mathbf{G}$ can be well estimated, sophisticated array signal processing algorithms can be later invoked to extract the information of interest from $\mathbf{G}$, e.g., the parameters like angles and reflection coefficients can be extracted from $\mathbf{G}$ via the MUSIC and APES algorithms.

The 3-rd Paragraph of Page 4:

For the upstream task here, the key is to optimize transmit waveform $\mathbf{X}$, which makes the estimation of $\mathbf{G}$ both accurate and simple. Given the linear signal model $\mathbf{Y}_{\mathrm{R}} = \mathbf{G}\mathbf{X} + \mathbf{Z}_{\mathrm{R}}$, an estimator of $\mathbf{G}$, which is calculated easily, can be obtained via the pseudo-inverse method, i.e., $\hat{\mathbf{G}} = \mathbf{Y}_{\mathrm{R}}\mathbf{X}^{\mathrm{H}}\big(\mathbf{X}\mathbf{X}^{\mathrm{H}}\big)^{-1}$. It can be verified that the estimator $\hat{\mathbf{G}}$ is unbiased, i.e., $\mathbb{E}(\hat{\mathbf{G}}) = \mathbf{G}$, with mean square error (MSE) $N_{\mathrm{R}}\sigma_{\mathrm{R}}^2\mathrm{tr}\big(\mathbf{X}\mathbf{X}^{\mathrm{H}}\big)^{-1}$. It can also be verified that the MSE of $\hat{\mathbf{G}}$ and the CRB of $\mathbf{G}$ coincide, which shows that the estimator is efficient and, in some sense, optimal [45], as the MSE attains CRB. Hence, the design goal in this paper is to optimize $\mathbf{X}$ by minimizing the MSE of $\hat{\mathbf{G}}$ or the CRB of $\mathbf{G}$ subject to the constraints on communication quality and transmit power, which can be formulated as

$$\begin{aligned} \min_{\mathbf{X}} \quad & \mathrm{tr}\big((\mathbf{X}\mathbf{X}^{\mathrm{H}})^{-1}\big) \\ \text{s.t.} \quad & \big|\mathrm{Im}(\mathbf{h}_u^{\mathrm{H}}\mathbf{x}_l e^{-j\xi_{u,l}})\big| \leq \\ & \qquad \big(\mathrm{Re}(\mathbf{h}_u^{\mathrm{H}}\mathbf{x}_l e^{-j\xi_{u,l}}) - \gamma_u\big)C_\pi, \ (\forall\, u, l) \\ & \|\mathbf{x}_l\|^2 \leq p, \ (\forall\, l), \end{aligned} \tag{7}$$

where p denotes the maximum transmit power for each symbol vector, and $C_\pi = \tan(\pi/D)$.

Comment 4:

4. 3) Minor: Is the complexity of calculating $\mathbf{A}_l$ in the recursive algorithm considered? Further, an interesting work on two target CRLB is available here https://ieeexplore.ieee.org/document/8537943.

Response:

Thank you very much for your detailed review. In fact, the terms N_{T}^3 and LN_{T}^2 in the complexity analysis are partly caused by the calculation of $\mathbf{A}_l$. Also, many thanks for sharing with us this high-quality paper, which really inspires us a lot. For example, although we cannot incorporate $\mathbf{G}$ explicitly in our approach temporarily (because of the reasons mentioned above), it inspires us to focus on or choose some specific practical parameters and design the corresponding algorithms. This will surely be our future work. Following your comment, we have updated our paper as follow:

The last Paragraph of Section IV (Page 10):

... Hence, the overall complexity is $\mathcal{O}\big((I+1)N_{\mathrm{T}}^3 + (IN+L)N_{\mathrm{T}}^2 + 2INN_{\mathrm{T}} + 4INKUN_{\mathrm{T}}\big)$.
...

Conclusion (Page 13):

... The future works include developing efficient parallelizable and recursive algorithms for general DFRC beamforming problems, general deep unfolding methods and efficient DFRC algorithms that exploit features from both communication and radar sensing and investigating DFRC algorithms by choosing specific parameters (like angle and velocity) as sensing metrics and optimizing the CRB.

Thanking you again for your generosity with your precious time, SINCERELY!

Jianjun Zhang, Christos Masouros, Fan Liu, Yongming Huang and A. Lee Swindlehurst

IEEE Journal of Selected Topics in Signal Processing
Paper ID: J-STSP-SPISC-00082-2023.R1
Authors' Response to Reviewer 1

We would like to thank you for your insightful suggestions and comments, which have helped us improve the quality of our paper. We have revised our paper incorporating all your suggestions and comments.

Comment 1:

1. The authors have satisfactorily addressed my concerns from the first round of the review. Given their deep unfolding approach and the (fractional) quadratic objective has similarities with other works in deep unfolding for radar, I'd suggest they consider including related works in their literature review. For instance:

[*] Metwaly, Kareem, et al. "Interpretable, Unrolled Deep Radar Beampattern Design." ICASSP 2023-2023 IEEE International Conference on Acoustics, Speech and Signal Processing (ICASSP). IEEE, 2023.

[*] Kang, Bosung, et al. "Deep Learning for Radar Waveform Design: Retrospectives and the Road Ahead." 2023 IEEE International Radar Conference (RADAR). IEEE, 2023.

[*] Khobahi, Shahin, et al. "Deep radar waveform design for efficient automotive radar sensing." 2020 IEEE 11th Sensor Array and Multichannel Signal Processing Workshop (SAM). IEEE, 2020.

Response:

We are very grateful to you for sharing with us these papers, which help us better understand deep unfolding and its applications. In the revised manuscript, we have included these excellent works in the literature review and updated our manuscript as follows:

The 4-th Paragraph of Left Column of Page 2:

... To reduce the complexity, deep unfolding approach has been investigated and exploited in various radar applications [41]-[43]. In [41], the state-of-the-art algorithm designed via projection, descent, and retraction operations is unfolded to generate a deep network to address the problem of radar beam-pattern design.

References (Page 15):

[41] K. Metwaly, J. Kweon, K. Alhujaili, M. Greco, F. Gini, and V. Monga, "Interpretable, unrolled deep radar beampattern design," in 2023 IEEE International Conference on Acoustics, Speech and Signal Processing (ICASSP), 2023, pp. 1-5.

[42] B. Kang, J. Kweon, M. Rangaswamy, and V. Monga, "Deep learning for radar waveform design: Retrospectives and the road ahead," in 2023 IEEE International Radar Conference (RADAR), 2023, pp. 1-6.

[43] S. Khobahi, A. Bose, and M. Soltanalian, "Deep radar waveform design for efficient automotive radar sensing," in 2020 IEEE 11th Sensor Array and Multichannel Signal Processing Workshop (SAM), 2020, pp. 1-5.

Thanking you again for your generosity with your precious time, SINCERELY!

Jianjun Zhang, Christos Masouros, Fan Liu, Yongming Huang and A. Lee Swindlehurst

IEEE Journal of Selected Topics in Signal Processing
Paper ID: J-STSP-SPISC-00082-2023.R1
Authors' Response to Reviewer 2

We would like to thank you for your insightful suggestions and comments, which have helped us improve the quality of our paper. We have revised our paper incorporating all your suggestions and comments.

Comment 1:

1, The paper titled "Low-Complexity Joint Radar-Communication Beamforming: From Optimization to Deep Unfolding" considered combining SLP with CRB. A serious design algorithm was proposed. It seems that the mathematical derivations are questionable. Additionally, the reviewer thinks that the considered ISAC system is quite arguable, which makes the motivation of this paper questionable. The optimization and learning methods are also typical. Therefore, the contribution of this paper is not clear enough.

Response:

Thank you very much for this comment. First of all, for your comment "the mathematical derivations are questionable", we would like to highlight that our mathematical derivations are correct and rigorous. We would like to refer you to the responses to Comments 10 and 11 for the details.

For your comment about ISAC system, we would like to refer you to the responses to Comments 6 and 8 for the details. We would like to explain that we have clarified and highlighted our motivation and contributions many times, and we would like to explain them once again. Our motivation is to address the challenging issue of prohibitive computational complexity when incorporating SLP and ISAC, and our main contributions are to develop multiple efficient parallelizable and recursive algorithms, from the point of view of both optimization and learning. For the sake of convenience, we would like to list our contributions (summarized in Section I of our paper) below:

- To exploit the multi-user interference and thus improve the energy efficiency of the DFRC system, we formulate the problem of joint radar-communication beamforming design based on SLP and, particularly, incorporate CI constraints into the problem of interest.
- To address the resulting non-convex optimization problem, we propose an efficient parallelizable iterative optimization algorithm, which can exploit latent separability of the optimization problem. We show that the proposed algorithm converges a locally optimal stationary point.
- In view of the space-time processing feature, we propose the idea of recursive optimization for SLP-based DFRC beamforming. For the considered problem, we propose an efficient recursive algorithm and reveal useful insights. In particular, we mathematically show that the proposed recursive algorithm monotonically improves the performance metric as the recursion proceeds.

- To further reduce the complexity, we propose efficient learning-based algorithms using deep-unfolding. Specifically, we first create unfolding-friendly iterative algorithms, and then unfold them by choosing the step-size parameters as the learnable parameters. In contrast to most learning-based algorithms, our algorithms enjoy the advantage of low training- and sample-complexity.

Finally, we would like to highlight that the most important goal of our manuscript is to address the real challenge - the large computational complexity, which has already limited the use of "useful algorithms", rather than focusing on "non-typical algorithms". Moreover, even following the criterion that the methods should be non-typical, we still provide novel idea and solutions. For example, we, for the first time, propose the idea of recursive optimization for the ISAC system, design efficient algorithms and prove the strict monotonicity of the algorithms. We hope that the Reviewer could give attention to these aspects, acknowledge our contributions and make an objective judgement.

Comment 2:

2. This paper seems to simply combine SLP and CRB for ISAC, which makes the considered problem simple enough. However, the integrated gain achieved by combining these two technologies is not discussed. Therefore, the considered system is quite arguable and just simply combines.

Response:

We very much appreciate the comment. We have clarified and highlighted in the previous response letter that the problem considered in this paper is very challenging due to the large computational complexity. We would like to present our analysis and list the main reasons below once again:

- In contrast to conventional beamforming or precoding designs for communications only, where the optimization variables take the form of vector, the optimization variables are matrices of large dimension in DFRC waveform optimization. In particular, the scale of optimization variable is proportional to the length of communication frame, which may be very large.

- Besides the size of the optimization variable, the scale of an optimization problem includes also the number of constraints. Unfortunately, the number of constraints in our problem is $U \times L$ (with U and L denoting the number of users and the length of communication frame, respectively). Since L can be very large, the scale of our problem can also be very large.

- It is known that the degree of difficulty of solving an optimization problem heavily depends on the scale of the problem. [4] Because of the reasons above, the optimization problem considered in our manuscript is challenging. Moreover, our objective function is highly nonlinear, which further increases the computational complexity.

- Last but not least, in contrast to an optimization problem with low requirement of real-time, which is allowed to be solved in a long time (e.g., a network layer optimization problem), the beamforming or precoding problem has to be solved in a very short time. As a result, the large computational complexity makes it challenging to implement in real-time.

[4]For example, even for the linear programming, it can still prevent real-time application if its scale is too large.

Because of the reasons above, the issue of large computational complexity has been an obstacle of applying advanced signal processing algorithms in ISAC, which motivates us to develop low-complexity solutions in this paper. Besides the contribution of problem formulation which incorporates the CI constraints into the DFRC waveform optimization for the first time, our most important contributions are to develop multiple efficient parallelizable and recursive algorithms, from the point of view of both optimization and learning. In particular, we develop efficient parallelizable beamforming algorithms (which also apply to more general SLP problems) and, for the first time, propose efficient recursive beamforming algorithms. The idea underlying the recursive solution is tailored for ISAC, as the design or optimization along the time dimension is a typical feature of ISAC.

The integrated gain achieved by our proposal is, at least, three-fold. First, higher energy efficiency or, equivalently, spectrum efficiency can be achieved thanks to the SLP scheme. In fact, it may be a well-known fact that SLP can significantly save the transmit power by exploiting the constructive interference, to achieve the same or better transmission performance [R1]-[R7]. Second, compared to the BLP (block-level precoding) based ISAC designs (e.g., the algorithm in [23]), better sensing performance and performance tradeoff can be achieved. Last but not least, still compared to the BLP based works, our algorithms also enjoy the advantage of lower computational complexity.

[R1] A. Li, D. Spano, J. Krivochiza, S. Domouchtsidis, C. G. Tsinos, C. Masouros, S. Chatzinotas, Y. Li, B. Vucetic, and B. Ottersten, "A tutorial on interference exploitation via symbol-level precoding: Overview, state-of-the-art and future directions," IEEE Communications Surveys Tutorials, vol. 22, no. 2, pp. 796-839, 2020.

[R2] C. Masouros and E. Alsusa, "Dynamic linear precoding for the exploitation of known interference in MIMO broadcast systems," *IEEE Trans. Wireless Commun.*, vol. 8, no. 3, pp. 1396–1404, 2009.

[R3] C. Masouros, "Correlation rotation linear precoding for MIMO broadcast communications," *IEEE Trans. Signal Process.*, vol. 59, no. 1, pp. 252–262, 2011.

[R4] C. Masouros and T. Ratnarajah, "Interference as a source of green signal power in cognitive relay assisted co-existing MIMO wireless transmissions," *IEEE Trans. Commun.*, vol. 60, no. 2, pp. 525–536, 2012.

[R5] C. Masouros, T. Ratnarajah, M. Sellathurai, C. B. Papadias, and A. K. Shukla, "Known interference in the cellular downlink: a performance limiting factor or a source of green signal power?" *IEEE Commun. Mag.*, vol. 51, no. 10, pp. 162–171, 2013.

[R6] C. Masouros, M. Sellathurai, and T. Ratnarajah, "Vector perturbation based on symbol scaling for limited feedback MISO downlinks," *IEEE Trans. Signal Process.*, vol. 62, no. 3, pp. 562–571, 2014.

[R6] A. Li, D. Spano, J. Krivochiza, S. Domouchtsidis, C. G. Tsinos, C. Masouros, S. Chatzinotas, Y. Li, B. Vucetic, and B. Ottersten, "A tutorial on interference exploitation via symbol-level precoding: Overview, state-of-the-art and future directions," *IEEE Communications Surveys Tutorials*, vol. 22, no. 2, pp. 796–839, 2020.

[R7] C. Masouros and G. Zheng, "Exploiting known interference as green signal power for downlink

beamforming optimization," *IEEE Trans. Signal Process.*, vol. 63, no. 14, pp. 3628–3640, 2015.

Following your comment, we have updated our manuscript as follows:

The Last-But-One Paragraph of Page 2:

The integration gain of SLP and DFRC waveform optimization is at least three-fold, including better communication performance, sensing performance and performance trade-off, but with reduced computational complexity. Comprehensive simulation results are provided to demonstrate these advantages. ...

Comment 3:

3. The Sec. I Introduction is still not clear. The authors mentioned "one of the primary motivations for ISAC is to improve energy efficiency", as a result, the authors adopted the SLP. Why SLP is more energy efficiency than block-level precoding. Do any of your simulation results reflect this point?

Response:

We are very grateful to you for the helpful comment. First, we would like to clarify that the term "energy efficiency" here is a bit different from the commonly-used one that maximizes the ratio between achievable (sum-) rate and transmit power consumed, although their nature and final goal are the same. Essentially, SLP is created to improve energy by exploiting the interference (or more exactly, the constructive interference), which thus saves the transmit power and further improves the energy efficiency [R1]-[R7] (provided in the response to the previous comment). The principle that SLP saves transmit power via constructive interference has been extensively discussed in literatures, e.g., [R1] and [R7], where comprehensive simulation results (to improve energy efficiency via saving the transmit power) are provided. We would like to refer you to [R1]-[R7] or other references for the details. Following your comment, we have updated our manuscript as follows:

The 3-rd Paragraph of Left Column of Page 2:

... Typically, constructive interference (CI) is exploited to save the transmit power and therefore improve the energy efficiency. Examples using the concept of CI to improve communication system performance can be found in [30]-[36] ...

Comment 4:

4. The authors mentioned the "facilitate real-time implementation". However, from Figure 11, the reviewer found it hard to obtain this conclusion. Please improve this figure. From now point of view, the time is above 1s? Can this achieve real-time implementation?

Response:

We very much appreciate your detailed review and helpful suggestion. Temporarily, we still concentrate on theoretical research and thus, similar to almost all theoretical researchers, we evaluate our algorithms via computer simulations implemented via Matalb and Python languages on a general-purpose computer. As a result, many factors affect the real-time performance. A typical factor is

that Matlab and Python are the interpreted languages, which are known to suffer from low executive efficiency, when compared to the compiled languages such as C or C++. Another one is that the parallelizability of our algorithms cannot well release on a general-purpose computer.

But even so, we can still conclude the advantage of low complexity of our algorithms via complexity analysis and existing numerical results, which are expected to achieve good real-time performance on more appropriate platforms, e.g., FPGA (which is very good at massively parallel computing). First, the theoretical analysis shows the low computational complexity, which lays the foundation of practical good performance. Second, compared to the benchmark, whose elapsed time increases dramatically as size of problem scale increases, the time required by ALL our algorithms is almost linear with the size of problem scale and increases slow. Finally, although our optimization-based solutions cost relatively more time (but much less than that of the benchmark), the learning-based counterparts cost very little time - achieve millisecond level performance.

Following your suggestion, we have updated our manuscript as follows:

> The Last Paragraph of Section V (Page 13):
>
> ... Moreover, if the algorithms are implemented on an FPGA platform, which is very good at massively parallel computing, the potential of parallelizability of our algorithms can be well released and much better real-time performance is expected to be present.

Comment 5:

5. I admit the [R1] is a high-quality paper, and give many definitions and categories. However, the authors seem to simply follow the idea in this work. Why "As for a SINR-based design, it might fall into none of the three sub-categories." as replied in Comment 5? The reviewer feels confused and disagrees with this response.

Response:

We very much appreciate your insightful comment. We have read and reviewed many papers (e.g., [R8]-[R11]) and we still think that the idea and categories in [R1] (in our original response letter) are more appropriate because they accommodate many different algorithms and provide many insights. We would like to explain that the concept "SINR-based design" is pretty vague. Therefore, we could only respond to this comment according to our understanding. According to our new understanding after reading more papers, we think that a SINR-based design can fall into any of the three sub-categories, since different waveform optimization designs can contain SINR-based constraints.

[R8] J. A. Zhang, F. Liu, C. Masouros, R. W. Heath, Z. Feng, L. Zheng, and A. Petropulu, "An overview of signal processing techniques for joint communication and radar sensing," IEEE J. Sel. Topics Signal Process., vol. 15, no. 6, pp. 1295-1315, 2021.

[R9] F. Liu, C. Masouros, A. P. Petropulu, H. Griffiths, and L. Hanzo, "Joint radar and communication design: Applications, state-of-the-art, and the road ahead," *IEEE Trans. Commun.*, vol. 68, no. 6, pp. 3834–3862, 2020.

[R10] D. Ma, N. Shlezinger, T. Huang, Y. Liu, and Y. C. Eldar, "Joint radar-communication strategies for autonomous vehicles: Combining two key automotive technologies," *IEEE Signal*

Process. Mag., vol. 37, no. 4, pp. 85–97, 2020.

[R11] L. Zheng, M. Lops, Y. C. Eldar, and X. Wang, "Radar and communication coexistence: An overview: A review of recent methods," *IEEE Signal Process. Mag.*, vol. 36, no. 5, pp. 85–99, 2019.

Following your comment, we have updated our manuscript as follows:

> The Last Paragraph of Page 1:
>
> ... Among various research problems, joint waveform optimization (WO) is pivotal to pursuing a desired performance tradeoff by choosing a performance metric to be optimized and constructing appropriate constraints [6],[11],[14]-[16],[18],[19], from both communication (e.g., SINR based constraints) and radar sensing (e.g., estimation accuracy). Many desired waveforms can be obtained by optimizing the spatial precoders, and three typical types within the proposed methods reviewed in [6] are mutual-information-based WO [20], [21], waveform (or beam-pattern) similarity-based WO [6],[14] and estimation-accuracy-based WO [22]-[24] .

Comment 6:

6. As for the response to Comment 6, sometimes the authors say their contribution is SLP, sometimes is the extended target, and sometimes is large-scale. What is the real contribution? Please clearly summarize.

Response:

Thank you for this comment. We would like to copy our ORIGINAL response to Comment 6 below:

Thank you for this comment. First, we would like to highlight that the computational complexity is prohibitively high, not "very low". We have clarified and highlighted the challenges of our problem in the response to your first comment. For convenience, we would like to list them once again:

- In contrast to conventional beamforming or precoding designs for communications only, where the optimization variables take the form of vector, the optimization variables are matrices of large dimension in DFRC waveform optimization. In particular, the scale of optimization variable is proportional to the length of communication frame, which may be very large.
- Besides the size of the optimization variable, the scale of an optimization problem includes also the number of constraints. Unfortunately, the number of constraints in our problem is $U \times L$ (with U and L denoting the number of users and the length of communication frame, respectively). Since L can be very large, the scale of our problem can also be very large.
- It is known that the degree of difficulty of solving an optimization problem heavily depends on the scale of the problem. Because of the reasons above, the optimization problem considered in our manuscript is challenging. Moreover, our objective function is highly nonlinear, which further increases the computational complexity.
- Last but not least, in contrast to an optimization problem with low requirement of real-time, which is allowed to be solved in a long time (e.g., a network layer optimization problem), the

beamforming or precoding problem has to be solved in a very short time. As a result, the large computational complexity makes it challenging to implement in real-time.

We would like to highlight that the challenges of an optimization problem depend on not only its form (e.g., whether it is linear or nonlinear, convex or non-convex), but also its scale. The challenge caused by the scale of our problem has already been justified. As for the form, the semi-definite programming, successfully solving the BLP (block-level precoding) counterpart in [R1], fails to solve our problem due to the nonlinear objection function, which, to some extent, shows its difficulty.

[R1] F. Liu, Y.-F. Liu, A. Li, C. Masouros, and Y. C. Eldar, "Cramer-Rao bound optimization for joint radar-communication beamforming," IEEE Trans. Signal Process., vol. 70, pp. 240-253, 2022.

We would like to highlight that one of the most important contributions in our paper is to develop multiple efficient parallelizable and recursive beamforming algorithms, which alleviate or address the challenge in terms of real-time caused by the problem scale. However, SCA does not help to tackle the issue caused by the problem scale. Moreover, SCA is mainly used to solve the sub-problem during the process of designing a complete algorithm. Therefore, it is inappropriate to evaluate our algorithms from the view that whether the SCA is chosen to design an algorithm.

To summarize, the large computational complexity is an obstacle, which reasonably constitutes the motivation of our work. Following your comment, we have updated our manuscript as follows:

The 4-th Paragraph of Left Column of Page 2:

... The large computational complexity, caused by large problem scale and highly nonlinear form, is a key motivation of this paper.

It is clear that throughout the response we mainly emphasized the challenges of the problem considered, namely, the large computational complexity caused by large problem scale and highly nonlinear form. Therefore, our main contribution is the development of low-complexity algorithms. It is also clear that we NEVER EVEN MENTION "SLP" and "extended target" in the above response.

Comment 7:

7. As for the response to Comment 13, can you give some simulation results to support the proposed methods can scale to QAM? If else, you can remove relevant sentences.

Response:

Many thanks for this comment. We have, in fact, explained in detail that it is sufficient to replace the CI constraints for different modulations. Moreover, the performance curves obtained are similar as well. To avoid almost the same result, we have removed relevant sentences in the revised paper.

Comment 8:

8. As for the response to Comment 14, the reviewer still feels estimate $\mathbf{G}$ *is indeed impractical. The reviewer admits* $\mathbf{G}$ *contains the information of almost all parameters of interest. But in practice, we need to estimate the specific information instead of a meaningless* $\mathbf{G}$*. Can the matrix G guide real-world surveillance? Besides, when the authors derive the CRB, they still need the information*

$\mathbf{G}$ *to formulate (6). However as indicated by the authors, they intend to estimate* $\mathbf{G}$*. It is also confusing.*

Response:

We very much appreciate your detailed review. We would like to first respond to the the latter part of this comment - "Besides, when the authors derive the CRB, they still need the information G to formulate (6). However as indicated by the authors, they intend to estimate $\mathbf{G}$". We would like to take an example to explain the "confusion". The example is to compute the derivative of function $f(x) = bx$ with b a constant. For this example, we have $f'(x) = \lim_{\Delta x \to 0}(f(x+\Delta x) - f(x))/\Delta x = \lim_{\Delta x \to 0}(b(x+\Delta x) - bx)/\Delta x = \lim_{\Delta x \to 0}(b\Delta x)/\Delta x = b$. It can be observed that during the process although we use the variable x to compute $f'(x)$, the final result shows that the derivative function is independent to the variable x. Similarly, during the process of deriving the CRB expression, we may refer to matrix $\mathbf{G}$, but the CRB expression does not depend on $\mathbf{G}$. In fact, $\mathbf{G}$ is estimated via the received signal $\mathbf{Y}_{\mathrm{R}}(= \mathbf{G}\mathbf{X} + \mathbf{Z}_R)$ and our task is to design $\mathbf{X}$, so as to better estimate $\mathbf{G}$. For this purpose, we first derive the CRB expression of $\mathbf{G}$ and then minimize it.

We would like to explain that in this paper we choose to estimate matrix $\mathbf{G}$ (rather than some specific parameters) and try to improve its quality by optimizing matrix $\mathbf{X}$ for the following reasons:

- First and foremost, the BS often has no prior knowledge about the number of scatterers or targets and different applications or tasks often have different estimation goals. Therefore, it is difficult (and even impossible) to derive a general analytic expression of CRB.
- To derive an analytic expression of CRB for some specific parameters of interest (e.g., velocity and distance), the techniques used by the receiver often have to be taken into account, which inevitably complicates the design of transmit waveform and limits its application scope.
- If $\mathbf{G}$ can be estimated efficiently, sophisticated array signal processing algorithms can be later invoked to extract the information of interest from $\mathbf{G}$. As an example, parameters like angles and reflection coefficients can be extracted from $\mathbf{G}$ via the MUSIC and APES algorithms.

Because of the reasons above, similar to [23], we decouple or decompose a practical estimation task into two sub-tasks, i.e., the upstream task and downstream task. The upstream task considered in our paper is in charge of designing transmit waveform, while the downstream task is responsible for estimating the practical parameters of interest. Next, we would like to elaborate on the upstream task in our paper. Clearly, an important goal is to design the transmit waveform matrix $\mathbf{X}$, so as to make the estimation of $\mathbf{G}$ more accurate and simple. Given the linear received signal model $\mathbf{Y}_{\mathrm{R}} = \mathbf{G}\mathbf{X} + \mathbf{Z}_{\mathrm{R}}$, an estimator of $\mathbf{G}$, which is calculated easily, can be obtained via the pseudo-inverse method and is given by $\hat{\mathbf{G}} = \mathbf{Y}_{\mathrm{R}}\mathbf{X}^{\mathrm{H}}\big(\mathbf{X}\mathbf{X}^{\mathrm{H}}\big)^{-1}$. It can be verified that the estimator $\hat{\mathbf{G}}$ is unbiased, i.e., $\mathbb{E}(\hat{\mathbf{G}}) = \mathbf{G}$, with the mean square error (MSE) $N_{\mathrm{R}}\sigma_{\mathrm{R}}^2\mathrm{tr}\big(\mathbf{X}\mathbf{X}^{\mathrm{H}}\big)^{-1}$. We can also verify that the CRB and the MSE of $\hat{\mathbf{G}}$ coincide. This shows that the estimator is also optimal, as the MSE attains the CRB. Hence, it is natural to optimize $\mathbf{X}$ by minimizing the CRB or MSE.

Based on the above discussion, we hope that you could acknowledge the rationality of our problem formulation. Following your suggestion, we have updated our manuscript as follows:

The Last Paragraph of Page 3:

In many cases, the Cramér-Rao bound (CRB) of specific parameters of interest is chosen as the performance metric to characterize the sensing performance, e.g., the direction cosine and radial velocity are considered in [44]. But similar to [23], the CRB of $\mathbf{G}$, instead of specific parameters, is chosen as the performance metric and optimization goal here. Essentially, we decouple or decompose a practical estimation task into two sub-tasks, i.e., the upstream task and downstream task. The upstream task is in charge of designing the transmit waveform $\mathbf{X}$, while the downstream task is responsible for estimating the specific parameters of interest. Moreover, if necessary, the receiver techniques should also be taken into account in the downstream task to improve the estimation quality.

The 2-nd Paragraph of Page 4:

The reasons to decompose a practical estimation task into two sub-tasks are as follows. First and foremost, the BS often has no prior knowledge about the number of scatterers or targets and different applications often have different estimation objectives. Second, to derive an analytic expression of CRB for specific parameters, the techniques used by the receiver often have to be taken into account, which complicates the design of $\mathbf{X}$ and limits the application scope. Finally, if $\mathbf{G}$ can be well estimated, sophisticated array signal processing algorithms can be later invoked to extract the information of interest from $\mathbf{G}$, e.g., the parameters like angles and reflection coefficients can be extracted from $\mathbf{G}$ via the MUSIC and APES algorithms.

The 3-rd Paragraph of Page 4:

For the upstream task here, the key is to optimize transmit waveform $\mathbf{X}$, which makes the estimation of $\mathbf{G}$ both accurate and simple. Given the linear signal model $\mathbf{Y}_{\mathrm{R}} = \mathbf{G}\mathbf{X} + \mathbf{Z}_{\mathrm{R}}$, an estimator of $\mathbf{G}$, which is calculated easily, can be obtained via the pseudo-inverse method, i.e., $\hat{\mathbf{G}} = \mathbf{Y}_{\mathrm{R}}\mathbf{X}^{\mathrm{H}}\big(\mathbf{X}\mathbf{X}^{\mathrm{H}}\big)^{-1}$. It can be verified that the estimator $\hat{\mathbf{G}}$ is unbiased, i.e., $\mathbb{E}(\hat{\mathbf{G}}) = \mathbf{G}$, with mean square error (MSE) $N_{\mathrm{R}}\sigma_{\mathrm{R}}^2 \mathrm{tr}\big(\mathbf{X}\mathbf{X}^{\mathrm{H}}\big)^{-1}$. It can also be verified that the MSE of $\hat{\mathbf{G}}$ and the CRB of $\mathbf{G}$ coincide, which shows that the estimator is efficient and, in some sense, optimal [45], as the MSE attains CRB. Hence, the design goal in this paper is to optimize $\mathbf{X}$ by minimizing the MSE of $\hat{\mathbf{G}}$ or the CRB of $\mathbf{G}$ subject to the constraints on communication quality and transmit power, which can be formulated as

$$\begin{aligned} \min_{\mathbf{X}} \quad & \mathrm{tr}\big((\mathbf{X}\mathbf{X}^{\mathrm{H}})^{-1}\big) \\ \text{s.t.} \quad & \big|\mathrm{Im}(\mathbf{h}_u^{\mathrm{H}}\mathbf{x}_l e^{-j\xi_{u,l}})\big| \leq \\ & \qquad \big(\mathrm{Re}(\mathbf{h}_u^{\mathrm{H}}\mathbf{x}_l e^{-j\xi_{u,l}}) - \gamma_u\big)C_\pi, \ (\forall\, u, l) \\ & \|\mathbf{x}_l\|^2 \leq p, \ (\forall\, l), \end{aligned} \tag{8}$$

where p denotes the maximum transmit power for each symbol vector, and $C_\pi = \tan(\pi/D)$.

Comment 9:

9. Similar to comment 7, the authors mention the "extended target". However, the authors said $\mathbf{G}$ *represents the response of* V *targets of interest. This is indeed confusion. Please make the system model more clear (single extended target or multiple targets). BTW, only citing [23] without any real-world support makes the sensing G arguable.*

Response:

We are very grateful to you for your helpful comment. We would like to take three specific examples (which correspond to real-world scenarios) to explain the "confusion" [23]:

- Single Point Target: The target is modeled as an unstructured point that is far away from the BS, e.g., a UAV. In this case, V takes value 1, i.e., $V = 1$.
- Single Extended Target: In this case, the target is typically modeled as a surface with a large number of distributed point-like scatterers, such as a vehicle or a pedestrian moving on the road. In this case, V takes value greater than 1, i.e., $V > 1$.
- Multiple (Point) Targets: All targets are modeled as unstructured points that are far away from the BS, e.g., multiple UAVs. In this case, V also takes value greater than 1, i.e., $V > 1$.

We would like to explain that since we focus on $\mathbf{G}$ (which has incorporated various cases), there is indeed no need to distinguish the different scenarios in our paper. [5]

Following your comment, we have updated the manuscript as follows:

> The 3-rd Paragraph of Right Column of Page 3:
>
> ... Note that by changing value V in (3), response matrix $\mathbf{G}$ can characterize different scenarios. For clarity, we here take two specific examples to illustrate this point: 1) multiple point targets - V unstructured points that are far away from the BS like multiple UAVs; and 2) single extended target - the target is modeled as a surface with multiple distributed point-like scatterers, e.g., a vehicle moving on the road [23].

Comment 10:

10. As for the responses to Comments 17 and 25, the authors mention their method based on the "gradient projection method". But the authors indeed just replace the original function with its first-order derivation. This is not a "gradient projection method" at all. Anyhow, the "gradient projection method" is only valid for convex function. Please clearly clarify!

Response:

Thank you very much for this comment. We would like to correct the statement that "Anyhow, the gradient projection method is only valid for convex function". In particular, the gradient projection method is an effective method to solve the problem taking the following form [R1]:

$$\begin{aligned} \min_{\boldsymbol{x}} \quad & f(\boldsymbol{x}) \\ \text{s.t.} \quad & \boldsymbol{x} \in \mathcal{C}, \end{aligned} \tag{9}$$

[5] But for the case $V = 1$, we can design better algorithms because of the special form of target response matrix $\mathbf{G}$.

where $\mathcal{C}$ is a closed convex set. If the function $f(\boldsymbol{x})$ is convex, then the optimization problem is a convex problem. However it is a non-convex problem if $f(\boldsymbol{x})$ is not convex. In Section 2.3 of [R1], the author takes problem (9) as an example to elaborate on the principle and usage of gradient projection method and provides the convergence analysis as well. We would like to kindly remind the Reviewer that: 1) the assumption or requirement on the objective function $f(\cdot)$ is continuously differentiable, rather than convex, continuously convex differentiable or other conditions with convexity assumption; and 2) we have already provided the reference [R1] in the previous response letter and even pointed out the specific chapter/section and we hope the Reviewer could read it.

[R1] D. P. Bertsekas, *Nonlinear Programming*, 2nd ed. Athena Scientific, 1999.

We would like to clarify that besides the first-order approximation, a quadratic penalty term is also incorporated into the objection, which thus makes the gradient projection method applicable. For convenience, we would like to rewrite the problem solved in this paper:

$$\begin{aligned} \min_{\mathbf{X}} \quad & -\mathrm{Re}\big(\mathrm{tr}((\mathbf{X}_n\mathbf{X}_n^{\mathrm{H}})^{-2}\mathbf{X}_n\mathbf{X}^{\mathrm{H}})\big) + \frac{\rho_n}{2}\|\mathbf{X}-\mathbf{X}_n\|_{\mathrm{F}}^2 \\ \text{s.t.} \quad & \big|\mathrm{Im}(\mathbf{h}_u^{\mathrm{H}}\mathbf{x}_l e^{-j\xi_{u,l}})\big| \le \big(\mathrm{Re}(\mathbf{h}_u^{\mathrm{H}}\mathbf{x}_l e^{-j\xi_{u,l}}) - \gamma_u\big)C_\pi, \ (\forall\, u,l) \\ & \|\mathbf{x}_l\|^2 \le p, \ (\forall\, l). \end{aligned} \tag{10}$$

The problem in (10) can be EQUIVALENTLY written as

$$\begin{aligned} \min_{\mathbf{X}} \quad & \|\mathbf{X}-\mathbf{X}_n-\mathbf{C}_n/\rho_n\|_{\mathrm{F}}^2 \\ \text{s.t.} \quad & \big|\mathrm{Im}(\mathbf{h}_u^{\mathrm{H}}\mathbf{x}_l e^{-j\xi_{u,l}})\big| \le \big(\mathrm{Re}(\mathbf{h}_u^{\mathrm{H}}\mathbf{x}_l e^{-j\xi_{u,l}}) - \gamma_u\big)C_\pi, \ (\forall\, u,l) \\ & \|\mathbf{x}_l\|^2 \le p, \ (\forall\, l). \end{aligned} \tag{11}$$

For brevity, the feasible set of problem (11) is denoted by $\mathcal{F}$ (which is a closed convex set), i.e.,

$$\mathcal{F} = \big\{\mathbf{X}\,\big|\,\|\mathbf{x}_l\|^2 \le p, (\forall\, l), \quad \big|\mathrm{Im}(\mathbf{h}_u^{\mathrm{H}}\mathbf{x}_l e^{-j\xi_{u,l}})\big| \le \big(\mathrm{Re}(\mathbf{h}_u^{\mathrm{H}}\mathbf{x}_l e^{-j\xi_{u,l}}) - \gamma_u\big)C_\pi, (\forall\, u,l)\big\}.$$

Recall that the projection (denoted by $\boldsymbol{x}^\star$) of a point $\boldsymbol{x}$ on a closed convex set $\mathcal{C}$ is defined as $\boldsymbol{x}^\star \triangleq \mathrm{Proj}_{\mathcal{C}}(\boldsymbol{x}) = \arg\min_{\boldsymbol{y}\in\mathcal{C}} ||\boldsymbol{y}-\boldsymbol{x}||^2$ (Appendix B of [R1]). Hence, the solution of problem (11) and also the iteration format solving problem (7) in our paper can be expressed as:

$$\mathbf{X}_{n+1} = \mathrm{Proj}_{\mathcal{F}}(\mathbf{X}_n + \mathbf{C}_n/\rho_n). \tag{12}$$

The convergence can be obtained immediately according to Proposition 2.3.3 of [R1].

Following your suggestion, we have updated our manuscript as follows:

Proof of Theorem 1 (Page 5):

For brevity, the feasible set of problem (12), which is closed and convex, is denoted by $\mathcal{F}$, i.e.,

$$\mathcal{F} = \big\{\mathbf{X} \,\big|\, \|\mathbf{x}_l\|^2 \le p, (\forall\, l), \quad \big|\mathrm{Im}(\mathbf{h}_u^{\mathrm{H}}\mathbf{x}_l e^{-j\xi_{u,l}})\big| \le \big(\mathrm{Re}(\mathbf{h}_u^{\mathrm{H}}\mathbf{x}_l e^{-j\xi_{u,l}}) - \gamma_u\big)C_\pi, (\forall\, u, l)\big\}.$$

Then, problem (12) can be equivalently written as

$$\begin{aligned} \min_{\mathbf{X}} \quad & \|\mathbf{X} - \mathbf{X}_n - \mathbf{C}_n/\rho_n\|_{\mathrm{F}}^2 \\ \text{s.t.} \quad & \mathbf{X} \in \mathcal{F}. \end{aligned} \tag{13}$$

According to the definition of projection in a Euclidean space [a], the optimal solution of problem (13), denoted by $\mathbf{X}_{n+1}$, can be compactly expressed as

$$\mathbf{X}_{n+1} = \mathrm{Proj}_{\mathcal{F}}(\mathbf{X}_n + \mathbf{C}_n/\rho_n). \tag{14}$$

Under some step-size criterion or rule [b], the convergence of the iteration in (14) can be obtained immediately, e.g., by invoking Proposition 2.3.3 in [47].

[a] The projection of a point $\boldsymbol{x}$ on a closed convex set $\mathcal{C}$, denoted by $\boldsymbol{x}^\star$, is defined as $\boldsymbol{x}^\star \triangleq \mathrm{Proj}_{\mathcal{C}}(\boldsymbol{x}) = \arg\min_{\boldsymbol{y}\in\mathcal{C}} ||\boldsymbol{y} - \boldsymbol{x}||^2$ (Appendix B of [47]).

[b] Note that although the expression in (14) is brief and compact, a closed-form solution is still unavailable. Hence, an iterative algorithm has to be invoked to tackle it, which involves the step-size parameter. Various step-size rules have been available, such as the Armijo or Goldstein rules [47].

Comment 11:

11. As for the response to Comment 26, the authors indicate they are based on penalty dual decomposition (PDD). In my opinion, PDD is a double-loop optimization method. The reviewer does not see the double-loop in the manuscript. Please clarify. Besides, the reviewer thoroughly read [R1]-[R2]. The reviewer has not found the details about how PDD can obtain the optimal solution for non-convex problems. The convergence proof is still needed for the proposed methods.

Response:

We are very grateful to you for your detailed review. It is true that PDD is a double-loop method, in which the outer loop updates the penalty parameter and dual variables and the inner loop solves a primal (optimization) problem. Roughly speaking, there are two different strategies to solve the primal problem, i.e., to solve the problem exactly (to iterate enough times) and to solve the problem inexactly (to iterative several times to obtain some degree of accuracy). In many cases, the strategy of inexact solving can still achieve good performance (especially for the block-descent-based solver) but with much reduced complexity. It is also suitable for our recursive design, because our algorithm strictly monotonously decreases the objective function value as the recursive procedure proceeds. For rigorousness, we consider the exact solving manner in Algorithm 6 in the revised paper. But the inexact solving strategy is still utilized when unfolding it, so as to reduce the complexity.

[R1] Q. Shi and M. Hong, "Penalty dual decomposition method for nonsmooth nonconvex opti-

mization - Part I: Algorithms and convergence analysis," IEEE Trans. Signal Process., vol. 68, pp. 4108-4122, 2020.

[R2] Q. Shi, M. Hong, X. Fu, and T.-H. Chang, "Penalty dual decomposition method for nonsmooth nonconvex optimization - Part II: Applications," IEEE Trans. Signal Process., vol. 68, pp. 4242-4257, 2020.

The problem considered in [R1] and [R2] is rewritten below for convenience:

$$\begin{aligned} \max_{\mathbf{x}} \quad & F(\boldsymbol{x},\boldsymbol{y}) = f(\boldsymbol{x},\boldsymbol{y}) + \sum_{j=1}^{n_y} \tilde{\phi}(\boldsymbol{y}_j) \\ \text{s.t.} \quad & \boldsymbol{h}(\boldsymbol{x},\boldsymbol{y}) = \mathbf{0}, \quad \boldsymbol{g}_i(\boldsymbol{x}_i) \leq \mathbf{0}\,(i = 1, 2, \cdots, n). \end{aligned} \tag{15}$$

Note that for our problem, the non-smooth term $\sum_{j=1}^{n_y} \tilde{\phi}(\boldsymbol{y}_j)$ is absent. In [R1] and [R2], the objective function $f(\boldsymbol{x},\boldsymbol{y})$ is a continuously differentiable function and $\boldsymbol{g}_i(\boldsymbol{x}_i)$ is a vector of continuously differentiable functions. Note that the continuously differentiable functions can be non-convex and, in fact, many examples provided in [R2] are non-convex problems. Note also that PDD achieves a (locally) optimal solution for non-convex problems in this case. [6] Since [R1] has already provided the convergence proof, which also applies to our problem, there is no need to prove it again.

Following your comment, we have updated our manuscript as follows:

> The 3-rd Paragraph of Left Column of Page 10:
>
> ... Based on (38) - (43), problem (33) can be efficiently solved, with the complete procedure provided in Algorithm 6, which is a triple-loop iterative algorithm. The outer loop updates the parameter ξ, and the inner double-loop solves problem (35). ...

[6] By the way, we would like to kindly mention that the Robinson constraint qualification is considered in [R1], so as to accommodate the non-smooth terms. If the non-smooth terms are absent, the Robinson condition degenerates to the familiar Mangasarian-Fromovitz or even Slater constraint qualification. Accordingly, the convergence proof also takes the form of the analysis presented in many papers.

Algorithm 6 (Page 10):

Algorithm 6: Iterative Algorithm for Problem (29)

1: **initialize:** optimization variable $\mathbf{x}_0$ and parameter ξ_0; set counter $i = 0$

2: **repeat**

(a) **construct** optimization problem (34)

(b) **repeat** (to solve constructed problem)

(1) **repeat** (to solve primal problem)

1) **update x** as per (39) and (38)

2) **update z** by solving problem (40)

until some criterion is met

(2) **update** dual variable **y** as per (41)

(3) **update** parameter ρ according to (42)

until some convergence criterion is met

(c) **update** parameter ξ_{i+1} according to (43)

(d) **update** counter $i \leftarrow i + 1$

3: **until** some convergence criterion is met

4: **output:** optimal solution $\mathbf{x}^\star$

Thanking you again for your generosity with your precious time, SINCERELY!

Jianjun Zhang, Christos Masouros, Fan Liu, Yongming Huang and A. Lee Swindlehurst

IEEE Journal of Selected Topics in Signal Processing
Paper ID: J-STSP-SPISC-00082-2023.R1
Authors' Response to Reviewer 3

We would like to thank you for your insightful suggestions and comments, which have helped us improve the quality of our paper. We have revised our paper incorporating all your suggestions and comments.

Comment 1:

1. Regarding Comment 4, could you also incorporate your explanations into the paper:

"data $\mathbf{S}$ *is completely determined by the communication system (so that (7) optimizes the nonlinear mapping* $\mathbf{X}$ *for a given* $\mathbf{S}$*), and during the process we do not intervene in the operation of the communication system by controlling or modifying* $\mathbf{S}$ *in any way."*

Also this one:

"(7) optimizes the nonlinear mapping $\mathbf{X}$ *for a given* $\mathbf{S}$*"*

Response:

We are very grateful to you for your helpful suggestion, which helps the readers better understand our paper. In the revised manuscript, we have incorporated the explanation into our manuscript and, following your comment, we have updated the manuscript as follows:

> The 2-nd Paragraph of Section II (Page 3):
>
> ... Note that the data matrix $\mathbf{S}$ is completely determined by the communication system (so that the problem in (7) optimizes the nonlinear mapping $\mathbf{X}$ for a fixed $\mathbf{S}$), and during the process we do not intervene in the operation of the communication system by controlling or modifying $\mathbf{S}$ in any way.

Comment 2:

2. Regarding Comment 8, the authors state that:

"Based on (17), the algorithm designed to solve problem (16) converges to the same globally optimal solution of problem (13)"

To my understanding, you propose an algorithm to solve (17) (as written at the beginning of page 6), which converges to the same globally optimal solution of problem (16) and (13). Is that correct? Can you clarify that part a bit more?

Response:

We are very grateful to you for your astute query and valuable suggestion. We would like to clarify that the solution of problem (17) (in the previous version of our paper) is not the opitmal solution

of problem (16) (in the previous version of our paper). Then, to obtain the optimal solution of (16), we, in fact, solve a serial of optimization problems constructed according to (17), instead of only one problem taking the form of (17). The approximate or exact solutions [7] of these optimization problems constructed according to (17) converge to the optimal solution of problem (16). Because problem (16) is equivalent to problem (13) (in terms of $\mathbf{x}_l$) and both the two problems are convex, different iterative algorithms solved them yield the same optimal solution (still in terms of $\mathbf{x}_l$). [8] Following your suggestion, we have updated the manuscript as follows, to avoid possible confusion:

> The 2-nd Paragraph of Left Column of Page 6:
>
> ... By constructing a serial of sub-problems taking the form of (16) and solving them exactly or inexactly, these solutions finally converge to the same globally optimal solution of problem (15) or (12) in terms of $\mathbf{x}_l$.

Comment 3:

3. Regarding Comment 12, does the optimal $X^\star$ obtained by the optimization-based iterative algorithm represent the globally optimal solution? How can we justify the use of $X^\star$ as the ground-truth (or, globally optimal) solution against which to compare the proposed and benchmark deep learning schemes?

Response:

We very much appreciate your insightful comment. We would like to clarify that the solution $X^\star$ obtained by the optimization-based iterative algorithm is generally not globally optimal, but only locally optimal. For clarity, we would like to take the parallelizable design as an example to explain the relationship among different algorithms in Section III, their roles and their characteristics:

- Algorithm 1: It is designed to solve the non-convex optimization problem in (7). The solution obtained via this optimization algorithm is often locally optimal. [9]
- Algorithm 2: It is designed to solve a convex (and continuous) optimization in problem (13), which is constructed to solve problem (7). The solution obtained is globally optimal. [10]
- Algorithm 3: It is a learning-based algorithm derived from both Algorithms 1 and 2, which is designed to reduce their computational complexity.

[7] To obtain the optimal solution of problem (16), there is no need to exactly solve problem (17). Hence, we solve problems (18) and (19) only once in this paper. We would like to refer you to [R1] and [R2] for more details.
[R1] D. P. Bertsekas, Nonlinear Programming, 2nd ed. Athena Scientific, 1999.
[R2] Q. Shi and M. Hong, "Penalty dual decomposition method for nonsmooth nonconvex optimization - Part I: Algorithms and convergence analysis," IEEE Trans. Signal Process., vol. 68, pp. 4108-4122, 2020.

[8] By the way, we would like to clarify that the problem in (17) is just an approximate version of (16). Hence, the optimal solutions of the two problems are different.

[9] Note that it is often very difficult to obtain the globally optimal solution for a non-convex optimization problem.

[10] To obtain the globally optimal solution, some constraint qualification or condition, e.g., the well-known Slater's condition, should hold. But this condition is almost always met for a practical meaningful problem. Note that we design Algorithm 2 to address the challenge that the sub-algorithm within Algorithm 1 is not unfolding-friendly.

We would like to explain that we often evaluate an iterative optimization algorithm designed for a practical problem from two important aspects, namely: 1) the desired performance achieved by the algorithm; and 2) the computation resources required or consumed by the algorithm. Similar to many existing works (e.g., almost all deep-unfolding works, like [R1] - [R4], or the classical deep neural network based works, like [R5]), we also concentrate on the second aspect in this paper. In these works (e.g., [R3]-[R5]), since the iterative algorithms have a large computational complexity and the design goal of the learning-based counterparts is to reduce it, the solutions obtained via the iterative algorithms are chosen as the ground-truth, although they are just locally optimal. In our paper, we evaluate our learning-based algorithms in the same manner. In particular, they can achieve similar NMSE performance but with much reduced computational complexity.

[R1] V. Monga, Y. Li, and Y. C. Eldar, "Algorithm unrolling: Interpretable, efficient deep learning for signal and image processing," IEEE Signal Process. Mag., vol. 38, no. 2, pp. 18-44, 2021.

[R2] M. Borgerding, P. Schniter, and S. Rangan, "AMP-Inspired deep networks for sparse linear inverse problems," IEEE Trans. Signal Process., vol. 65, no. 16, pp. 4293-4308, 2017.

[R3] Q. Hu, Y. Cai, Q. Shi, K. Xu, G. Yu, and Z. Ding, "Iterative algorithm induced deep-unfolding neural networks: Precoding design for multiuser MIMO systems," IEEE Trans. Wireless Commun., vol. 20, no. 2, pp. 1394-1410, 2021.

[R4] K. Metwaly, J. Kweon, K. Alhujaili, M. Greco, F. Gini, and V. Monga, "Interpretable, unrolled deep radar beampattern design," in 2023 IEEE International Conference on Acoustics, Speech and Signal Processing (ICASSP), 2023, pp. 1-5.

[R5] H. Sun, X. Chen, Q. Shi, M. Hong, X. Fu, and N. D. Sidiropoulos,"Learning to optimize: Training deep neural networks for interference management," IEEE Trans. Signal Process., vol. 66, no. 20, pp. 5438-5453, 2018.

Following your comment, we have updated our manuscript as follows:

> The 2-nd Paragraph of Section V (Page 11):
>
> ... where $\hat{\mathbf{X}}$ denotes the transmit matrix predicted by algorithmic deep network and $\mathbf{X}^\star$ represents the transmit matrix obtained by optimization-based iterative algorithms in this paper, e.g., Algorithm 1 for the parallelizable design. Similar to [41]-[43],[55], since we concentrate on the reduction of computational complexity, it is appropriate to choose these possible locally optimal solutions as the benchmark or baseline.

Comment 4:

Regarding Comment 15: I think we are mixing up several things here. I would like to clarify them from my point of view and suggest the authors to do the same in the paper in the next round:

1) $\mathbf{G}$ *does not appear in the CRB optimization problem (7) because the CRB of* $\mathbf{G}$ *does not depend on* $\mathbf{G}$.

2) The reason why the CRB of $\mathbf{G}$ *does not depend on* $\mathbf{G}$ *is because* $\mathbf{G}$ *appears linearly in the received signal model (2) (unlike the case where the angles in (3) are estimated). Hence, the authors'*

statement "because the target response matrix $\mathbf{G}$ *(rather than some specific parameter of interest) is regarded as the parameter to be estimated, problem (7) does not depend on the form of* $\mathbf{G}$ *in (3) or the radar channel model." is not complete. The linearity of* $\mathbf{G}$ *in (2) is the main reason.*

3) "The reason for this consideration is three-fold." Here, the authors should provide clarification here by saying that "the reason for optimizing the CRB of $\mathbf{G}$ *instead of the CRB of the specific channel/target parameters in (7)". It is vague what "this consideration" refers to.*

4) Could you respond to my comment: "why do we even need to generate $\mathbf{G}$ *for the simulations?" Do the simulations depend on how you generate* $\mathbf{G}$*?*

Response:

We are very grateful to you for explaining this comment patiently. We are sorry for failing understanding your meaning. We would like to respond to these comments one by one.

1) We agree with you that $\mathbf{G}$ does not appear in the CRB optimization problem (7) (in the previous version of this paper) because the CRB of $\mathbf{G}$ does not depend on $\mathbf{G}$.

2) It is true that the absence of $\mathbf{G}$ in the CRB expression is mainly caused by the linear received signal model in (2), which makes the formulated problem more tractable.

3) Thank you very much for helping us polish our paper patiently and carefully. We are sorry for the vague statement, which may confuse the readers.

4) We would like to explain that because we choose the CRB as the performance metric to evaluate our algorithms and the benchmark or baseline in [23], there is indeed no need to generate matrix $\mathbf{G}$ in the simulations and the simulations also do not depend on how we generate $\mathbf{G}$. We are sorry that we even did not realize this important fact, and we thank you very much for your profound insight. Essentially, we decouple or decompose a practical estimation task into two sub-tasks, i.e., the upstream task and downstream task. The upstream task considered in our paper is in charge of designing the transmit waveform matrix $\mathbf{X}$, while the downstream task is responsible for estimating specific parameters of interest. This also accounts for the fact - why $\mathbf{G}$ is not needed.

By the way, we would like to explain in detail why we optimize the CRB of $\mathbf{G}$, rather than the CRB of some specific target parameters. Besides the reasons explained in the previous version, another important fact is that the CRB expression of specific target parameters also depends the receiver techniques, which greatly complicates the design of transmit waveform matrix $\mathbf{X}$ and also limits the application scope of our approach. But it is an interesting topic and is our future work.

Following your comment, we have updated our manuscript as follows:

The Last Paragraph of Page 3:

In many cases, the Cramér-Rao bound (CRB) of specific parameters of interest is chosen as the performance metric to characterize the sensing performance, e.g., the direction cosine and radial velocity are considered in [44]. But similar to [23], the CRB of $\mathbf{G}$, instead of specific parameters, is chosen as the performance metric and optimization goal here. Essentially, we decouple or decompose a practical estimation task into two sub-tasks, i.e., the upstream task and downstream task. The upstream task is in charge of designing the transmit waveform $\mathbf{X}$, while the downstream task is responsible for estimating the specific parameters of interest. Moreover, if necessary, the receiver techniques should also be taken into account in the downstream task to improve the estimation quality.

The 2-nd Paragraph of Page 4:

The reasons to decompose a practical estimation task into two sub-tasks are as follows. First and foremost, the BS often has no prior knowledge about the number of scatterers or targets and different applications often have different estimation objectives. Second, to derive an analytic expression of CRB for specific parameters, the techniques used by the receiver often have to be taken into account, which complicates the design of $\mathbf{X}$ and limits the application scope. Finally, if $\mathbf{G}$ can be well estimated, sophisticated array signal processing algorithms can be later invoked to extract the information of interest from $\mathbf{G}$, e.g., the parameters like angles and reflection coefficients can be extracted from $\mathbf{G}$ via the MUSIC and APES algorithms.

Footnote 8 (Page 11):

Note that because of the linear model in (2) and estimating $\mathbf{G}$, $\mathbf{G}$ is absent in the CRB expression. Hence, there is no need to generate matrix $\mathbf{G}$ in the simulations and the simulations also do not depend on how to generate $\mathbf{G}$.

Comment 5:

5. Regarding Comment 16: thanks for your response. I would like to correct two things:

(1) "MVUE estimator exists and is attainable". What do you mean by the "attainability" of an estimator? Do you mean that the RMSE of the MVUE attains the CRB?

(2) "its CRB is equal to the mean square error". The CRB is not tied to a specific estimator, so there is no such thing as "MVUE's CRB".

Response:

Thank you very much for your detailed review and patient reminder. For the first point, we would like to clarify that we do not mean that the RMSE of the MVUE attains the CRB. We mean that for a linear estimation model, the MVUE estimator of the parameter of interest exists, and its MSE is equal to the CRB of the parameter. For the second point, we thank you very much for correcting our original statement patiently. In the revised manuscript, we have rigorously distinguished the two concepts. Following your comment, we have updated the manuscript as follows:

The 3-rd Paragraph of Page 4:

For the upstream task here, the key is to optimize transmit waveform $\mathbf{X}$, which makes the estimation of $\mathbf{G}$ both accurate and simple. Given the linear signal model $\mathbf{Y}_{\mathrm{R}} = \mathbf{G}\mathbf{X} + \mathbf{Z}_{\mathrm{R}}$, an estimator of $\mathbf{G}$, which is calculated easily, can be obtained via the pseudo-inverse method, i.e., $\hat{\mathbf{G}} = \mathbf{Y}_{\mathrm{R}}\mathbf{X}^{\mathrm{H}}\left(\mathbf{X}\mathbf{X}^{\mathrm{H}}\right)^{-1}$. It can be verified that the estimator $\hat{\mathbf{G}}$ is unbiased, i.e., $\mathbb{E}(\hat{\mathbf{G}}) = \mathbf{G}$, with mean square error (MSE) $N_{\mathrm{R}}\sigma_{\mathrm{R}}^2 \mathrm{tr}\left(\mathbf{X}\mathbf{X}^{\mathrm{H}}\right)^{-1}$. It can also be verified that the MSE of $\hat{\mathbf{G}}$ and the CRB of $\mathbf{G}$ coincide, which shows that the estimator is efficient and, in some sense, optimal [45], as the MSE attains CRB. ...

Thanking you again for your generosity with your precious time, SINCERELY!

Jianjun Zhang, Christos Masouros, Fan Liu, Yongming Huang and A. Lee Swindlehurst